

Component separation for B-mode experiments

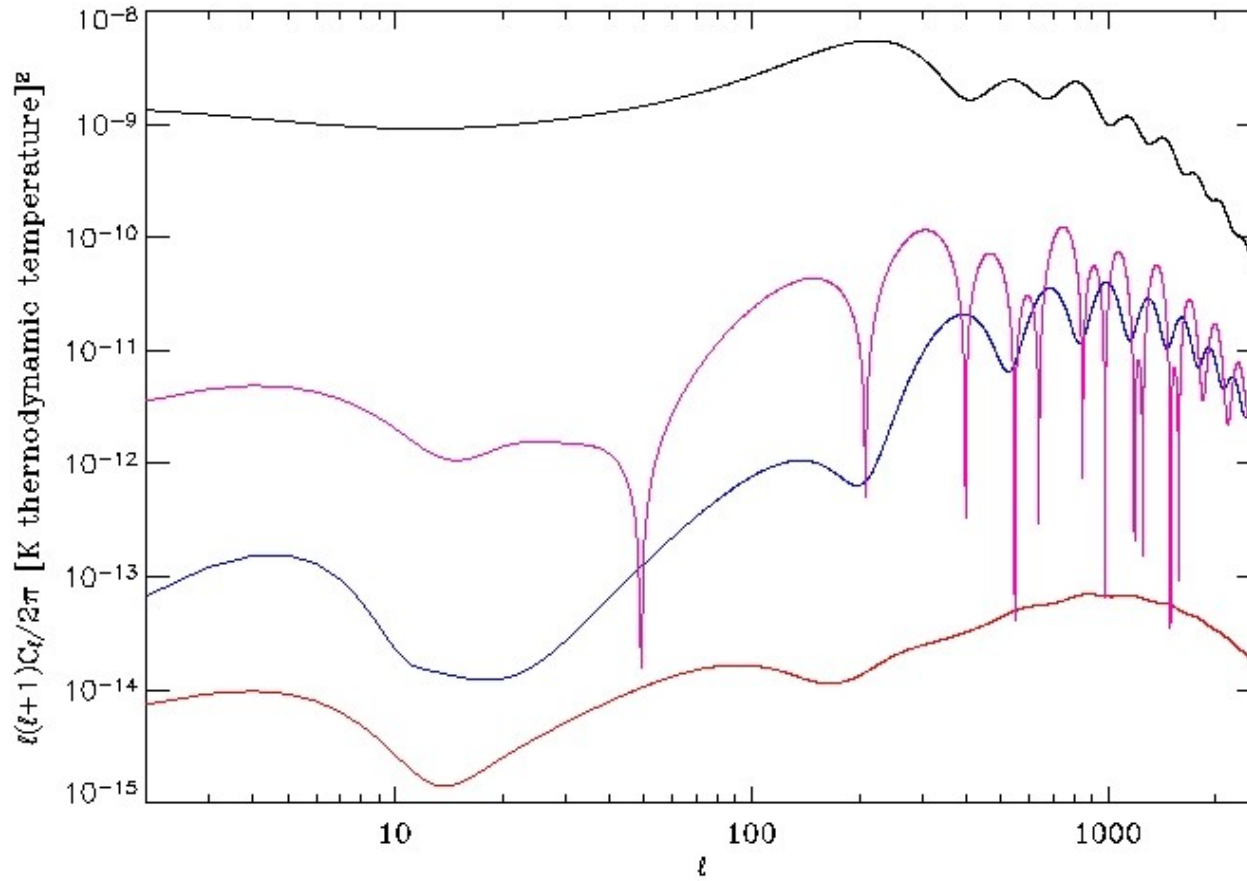
Carlo Baccigalupi
SISSA, Trieste
EWASS 2015



Outline

- Galactic foreground contamination to cosmological B-modes
- Status of observations
- Component separation
- Concluding remarks

CMB angular power spectrum

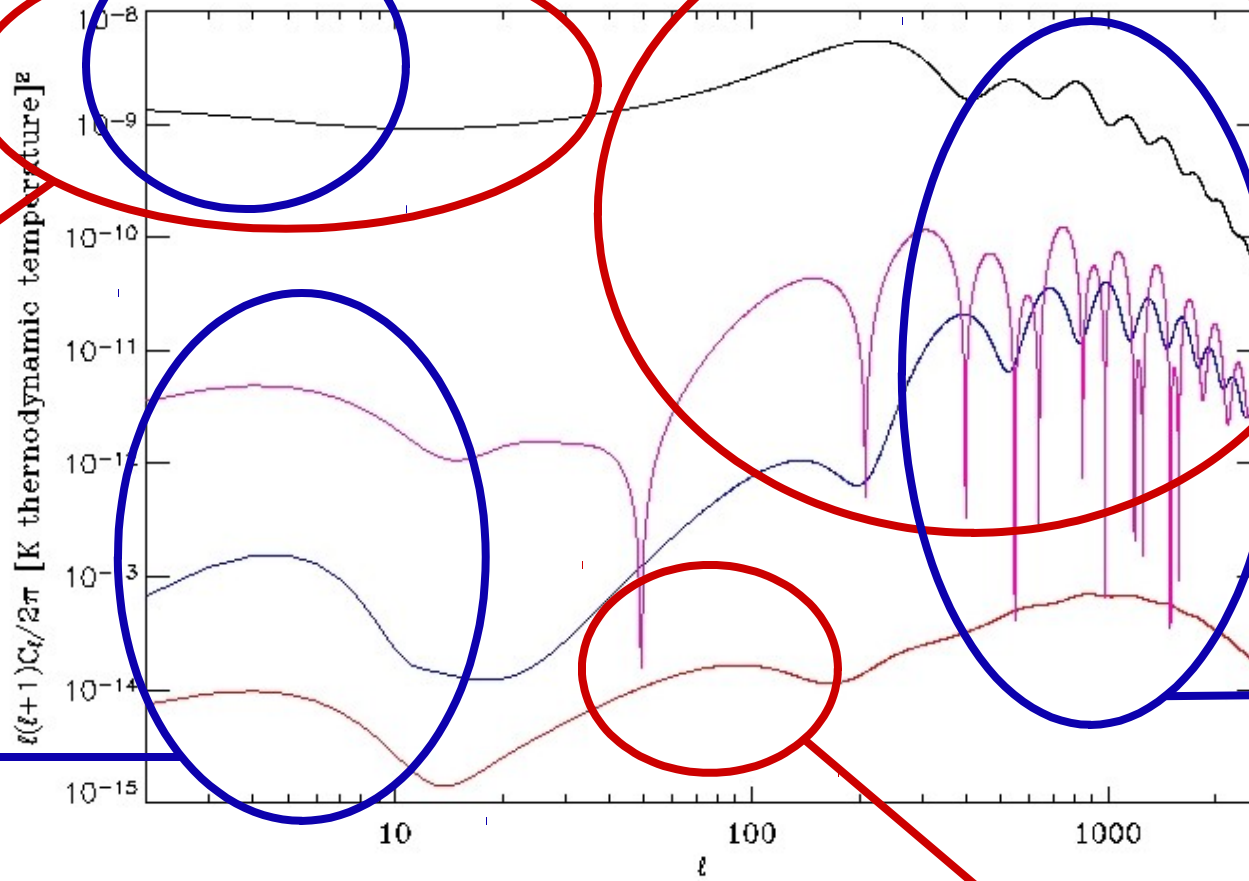


Angle $\approx 200/l$ degrees

CMB angular power spectrum

ISW

Acoustic oscillations



Angle $\approx 200/l$ degrees

Galactic foreground Contamination to cosmological B-modes



The scientific results that we present today are a product of the Planck Collaboration, including individuals from more than 100 scientific institutes in Europe, the USA and Canada

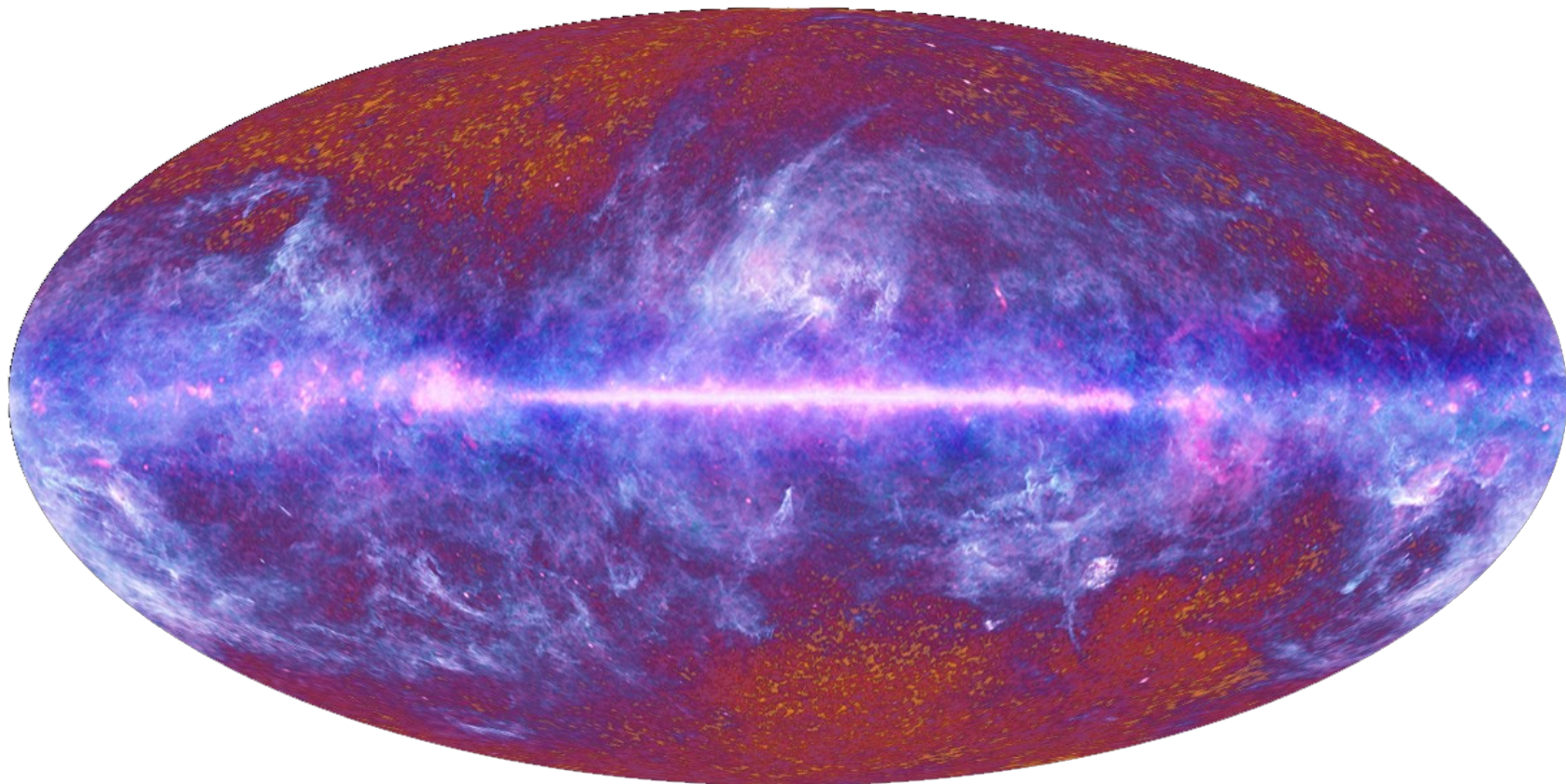


planck



Planck is a project of the European Space Agency, with instruments provided by two scientific Consortia funded by ESA member states (in particular the lead countries: France and Italy) with contributions from NASA (USA), and telescope reflectors provided in a collaboration between ESA and a scientific Consortium led and funded by Denmark.

$$F=A \text{ (sky direction)} \times F(\text{frequency})$$

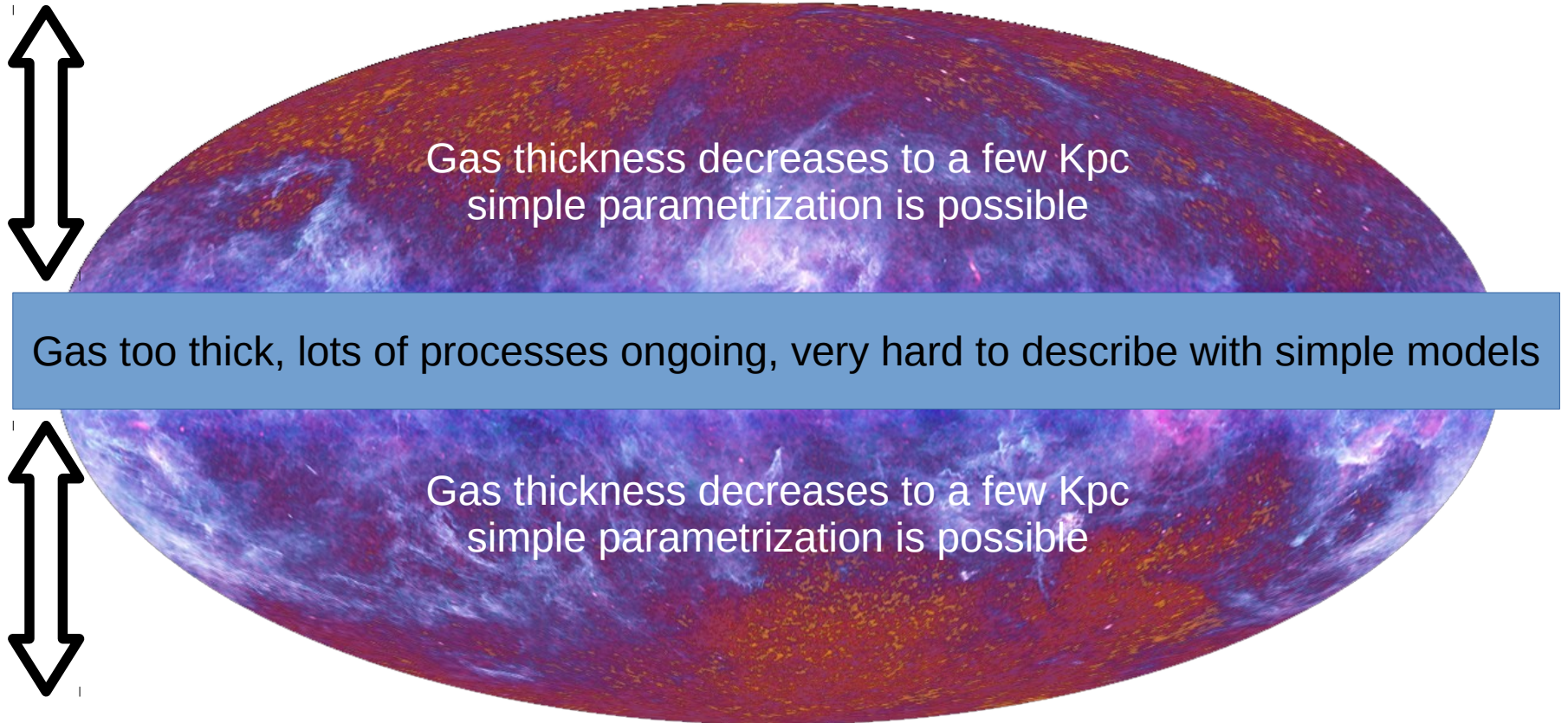


$$F=A \text{ (sky direction)} \times F(\text{frequency})$$



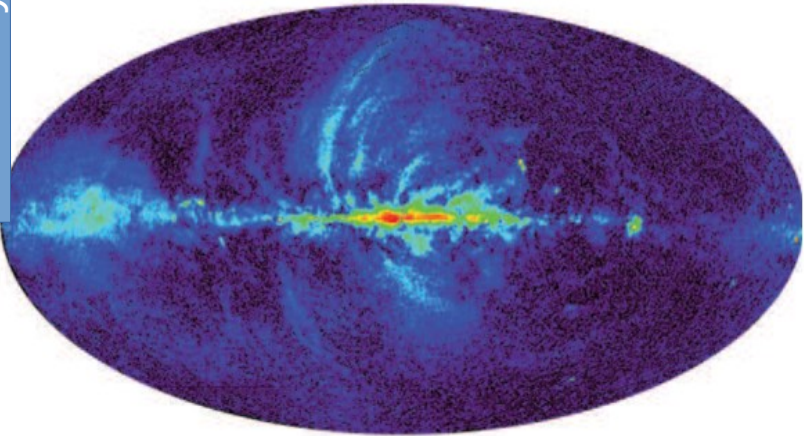
Gas too thick, lots of processes ongoing, very hard to describe with simple models

$$F=A \text{ (sky direction)} \times F(\text{frequency})$$

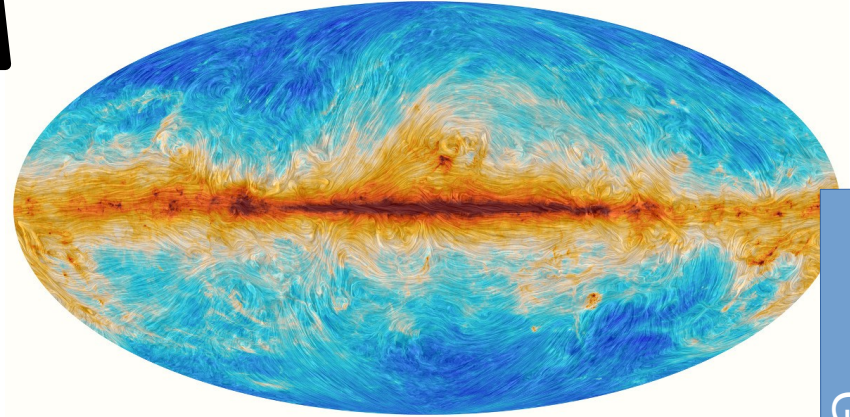


Galactic polarized foregrounds

Decaying power law



353 GHz

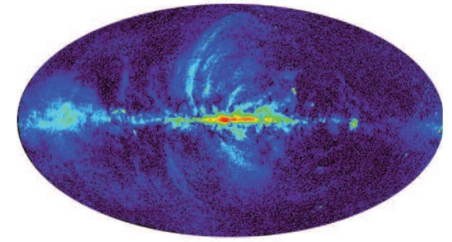


Grey body

23 GHz

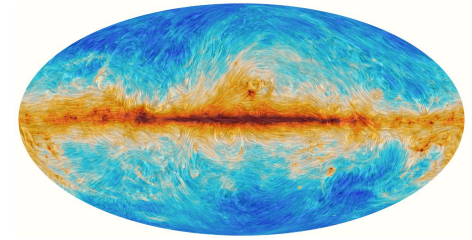


Polarized synchrotron



- Amplitude: cosmic ray electrons spiraling around the Galactic magnetic field
- Frequency scaling: approximate decaying power law frequency scaling ($F_{RJ} \sim f^{-3}$), determined by the electron distribution in energy
- Data: total intensity and polarization, several surveys at radio frequencies, WMAP and Planck at microwave frequencies
- Data at the required quality for B-mode cleaning: none

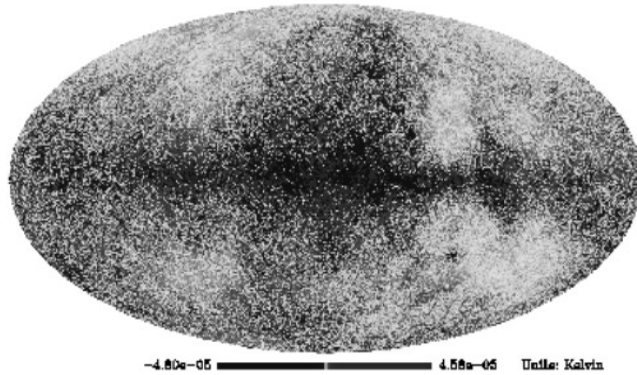
Polarized dust



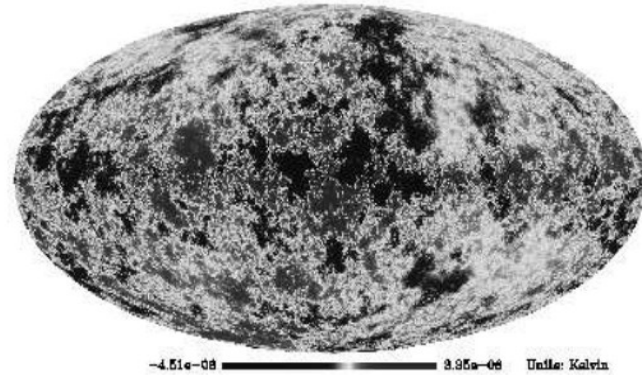
- Amplitude: magnetized dust grains emitting almost thermally, linearly polarized via local alignment with the Galactic magnetic field
- Frequency scaling: grey body $F_{RJ} \sim BB(f) \times f^{1.5}$
- Total intensity data: high resolution (few arcminutes) and sensitivity (IRAS and Planck) at 3000, 857, 545, 353 GHz for total intensity, degree scale mapping of temperature and emissivity
- Polarization data: Planck 2015 at 353 GHz
- Data at the required quality for B-mode cleaning: none

Foreground model building: the early days

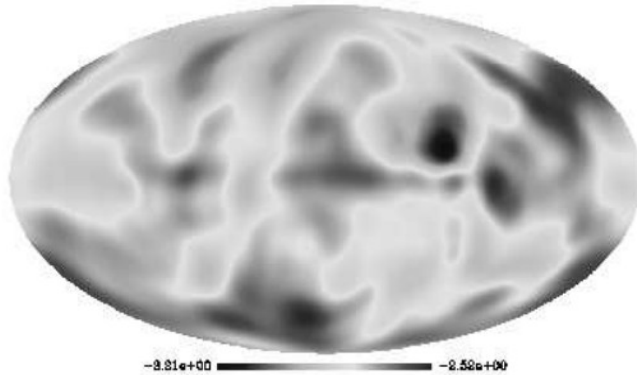
Modeled Q for synchrotron at 100 GHz (Gardino et al. 2002)



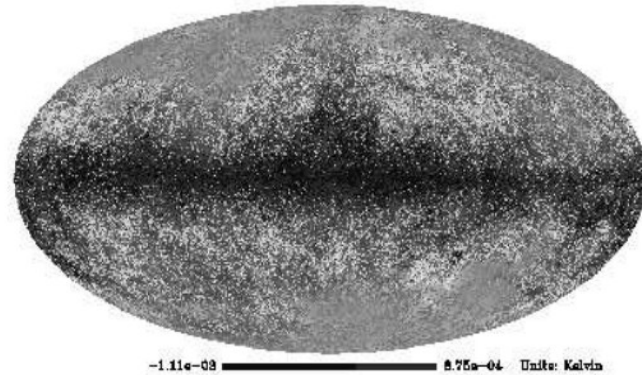
Modeled Q for synchrotron at 100 GHz (Baccigalupi et al. 2001)



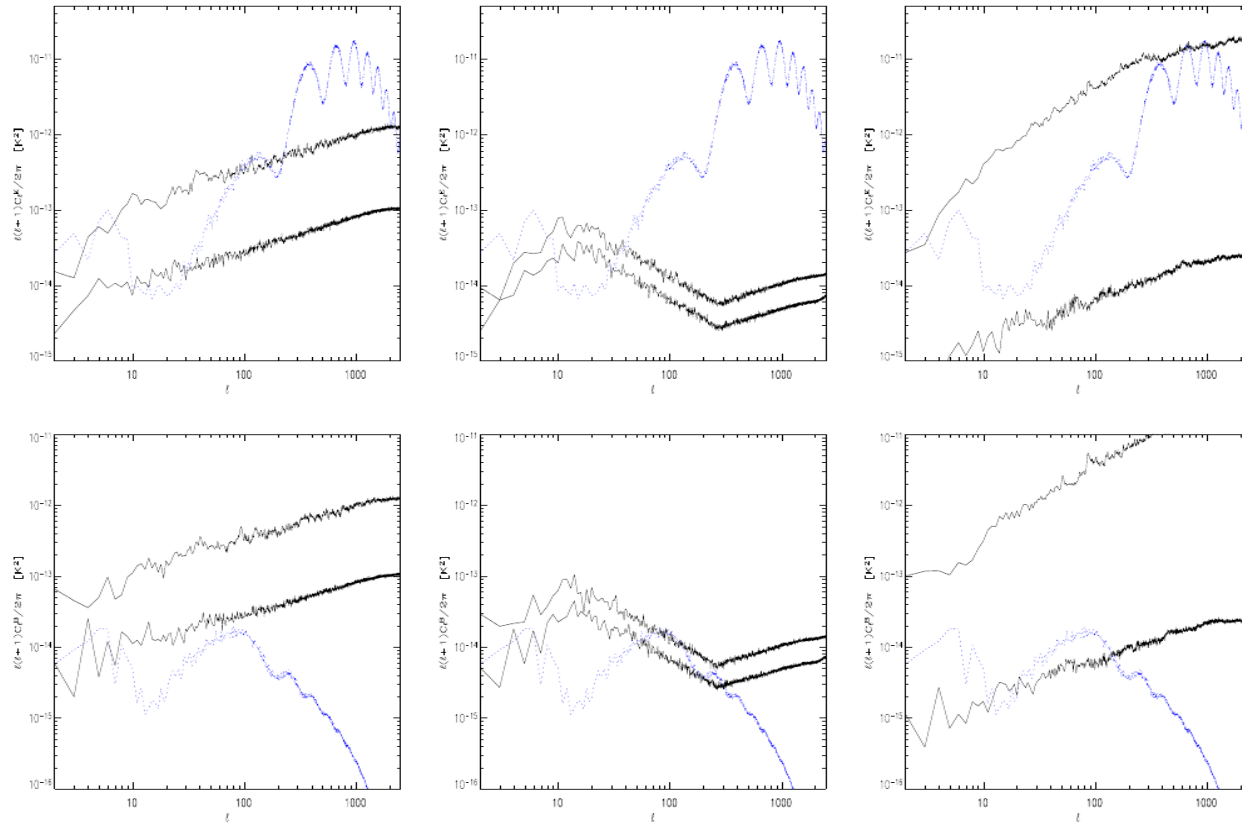
Synchrotron spectral index in antenna temperature



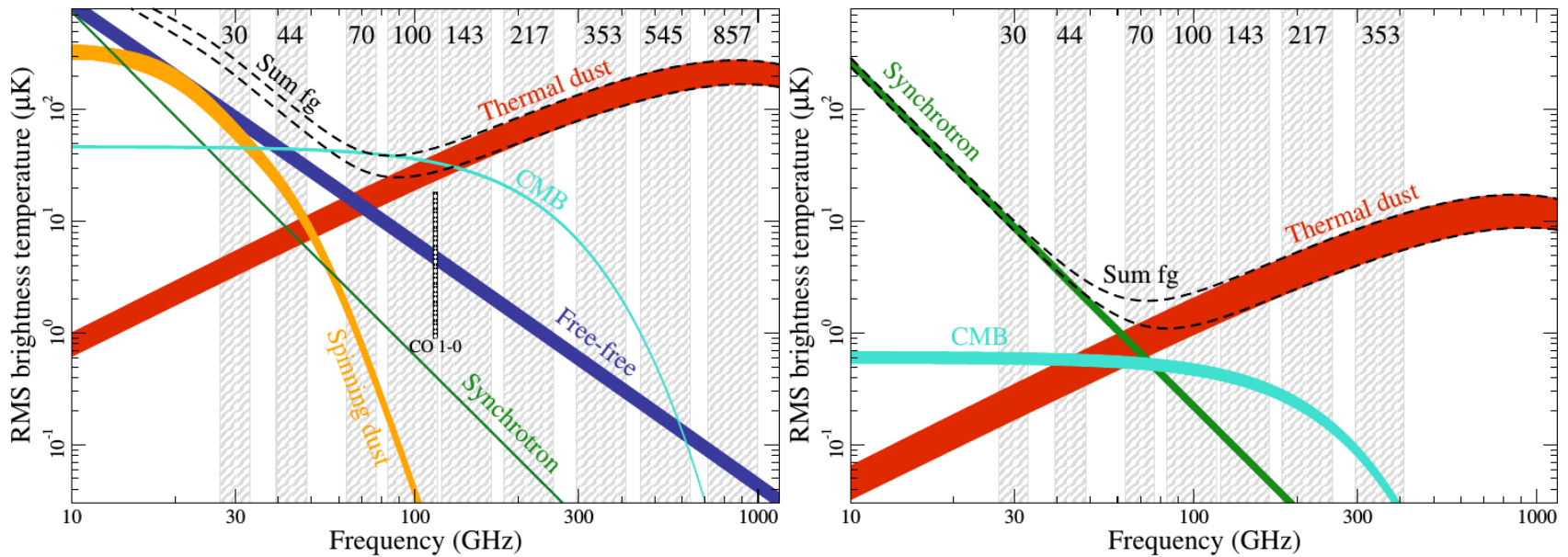
Modeled Q for dust at 100 GHz



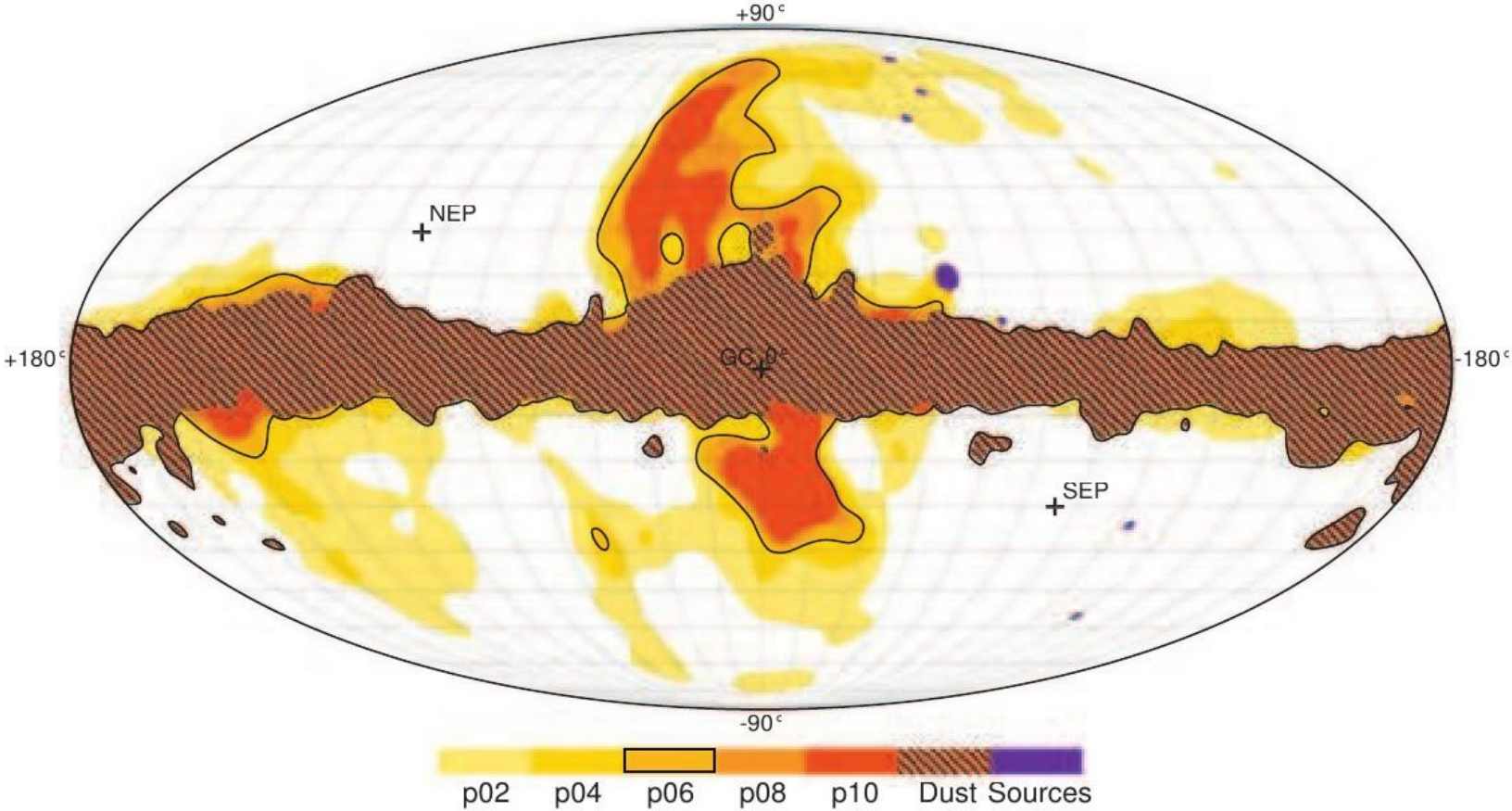
Foreground model building: the early days



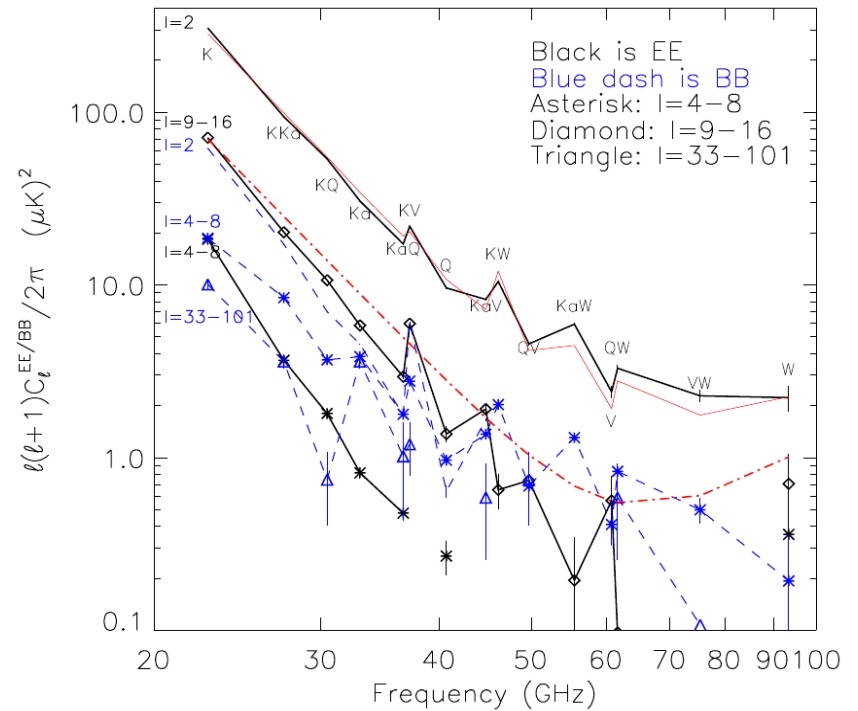
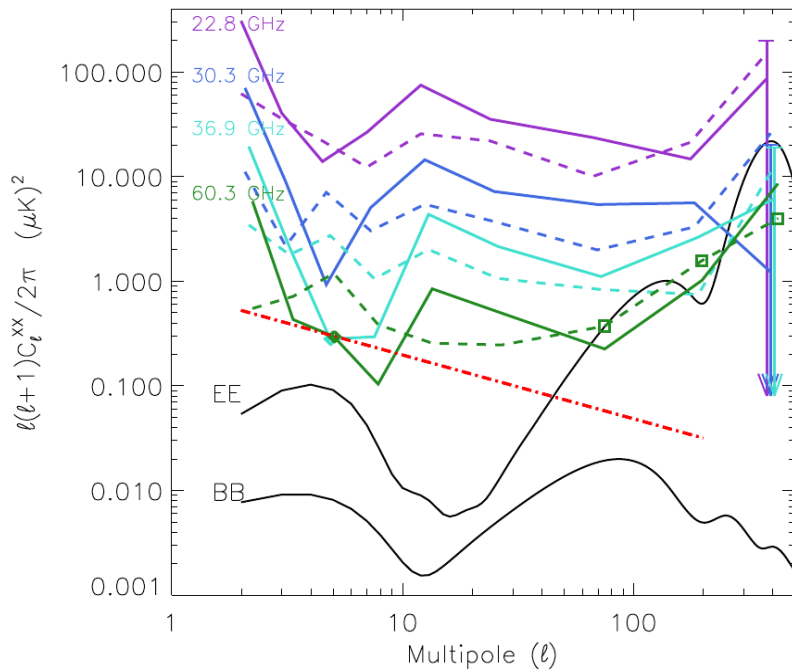
Foregrounds and frequency



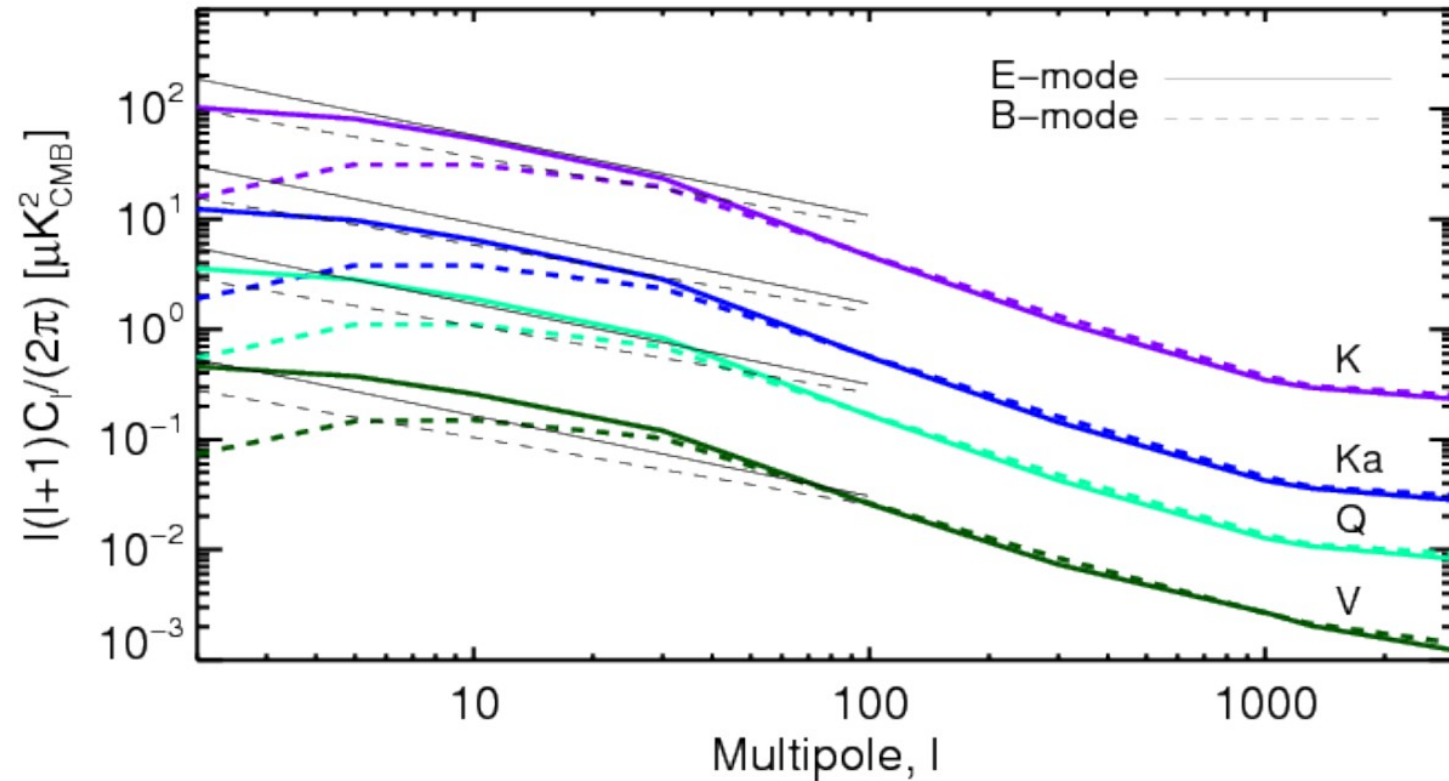
Observations: WMAP



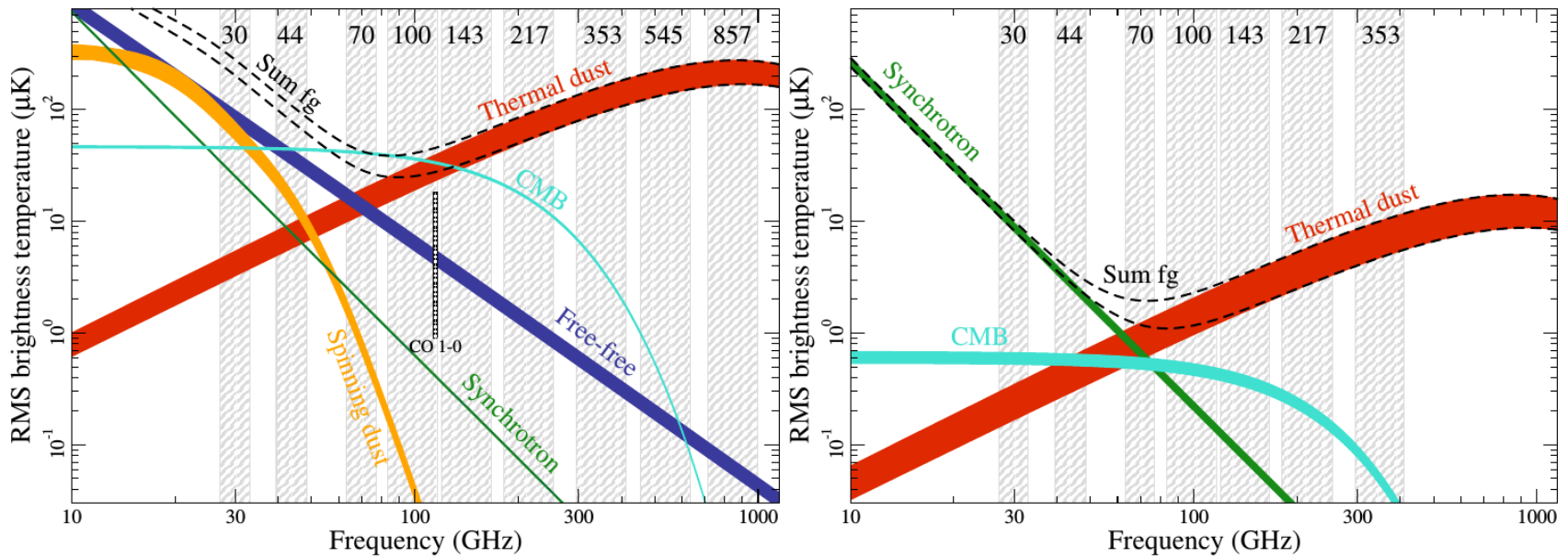
WMAP polarised foregrounds



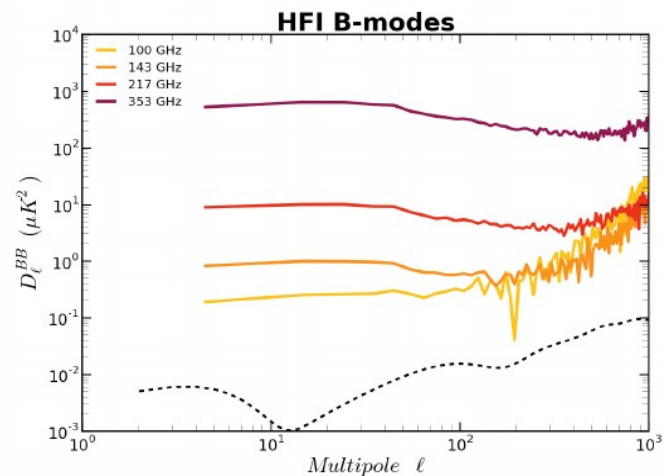
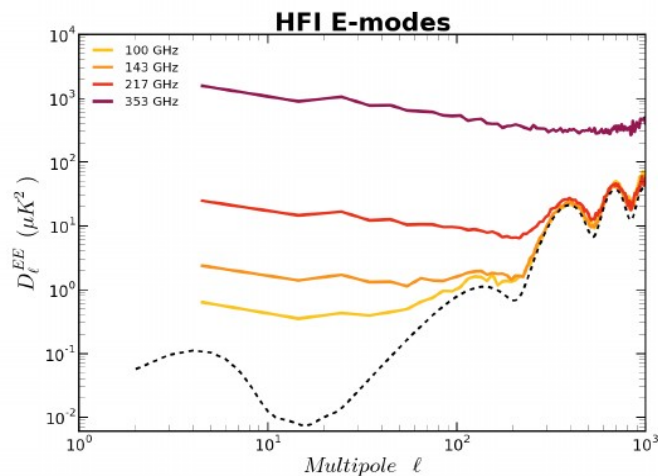
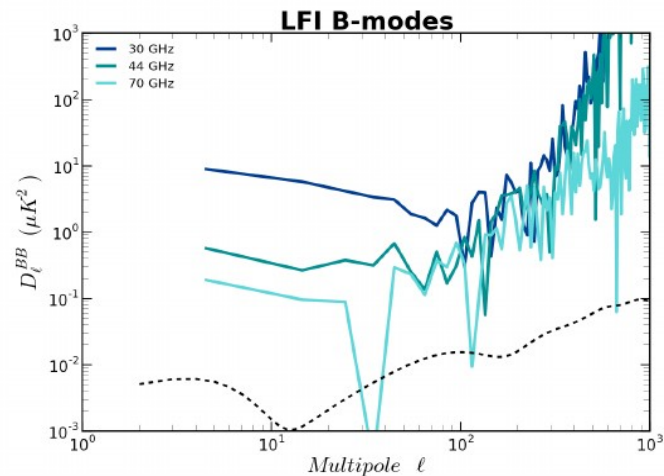
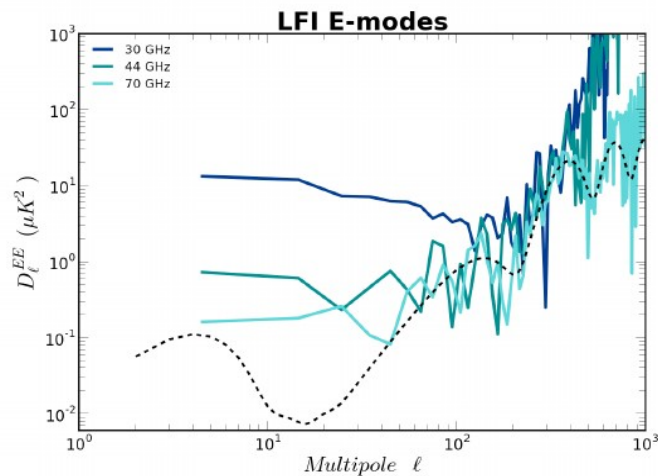
The (WMAP matching) Planck sky model



Foregrounds and frequency

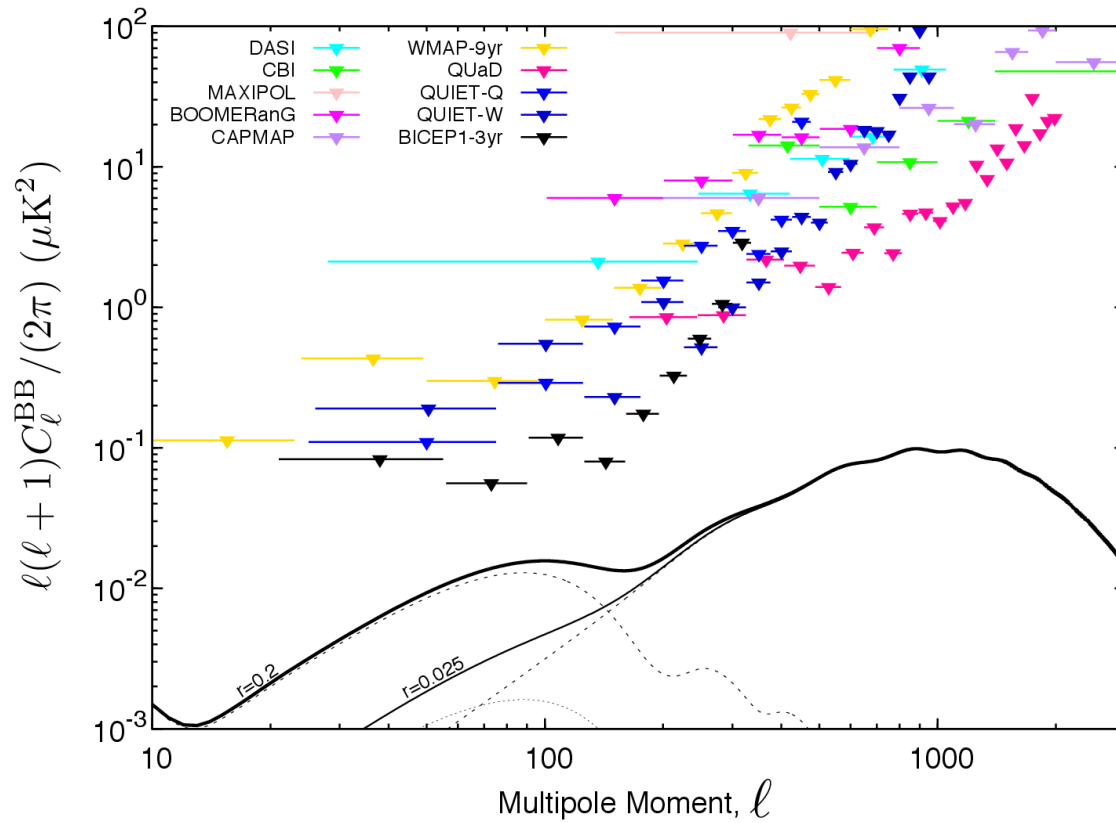


Planck foregrounds across multipoles with P06 masking

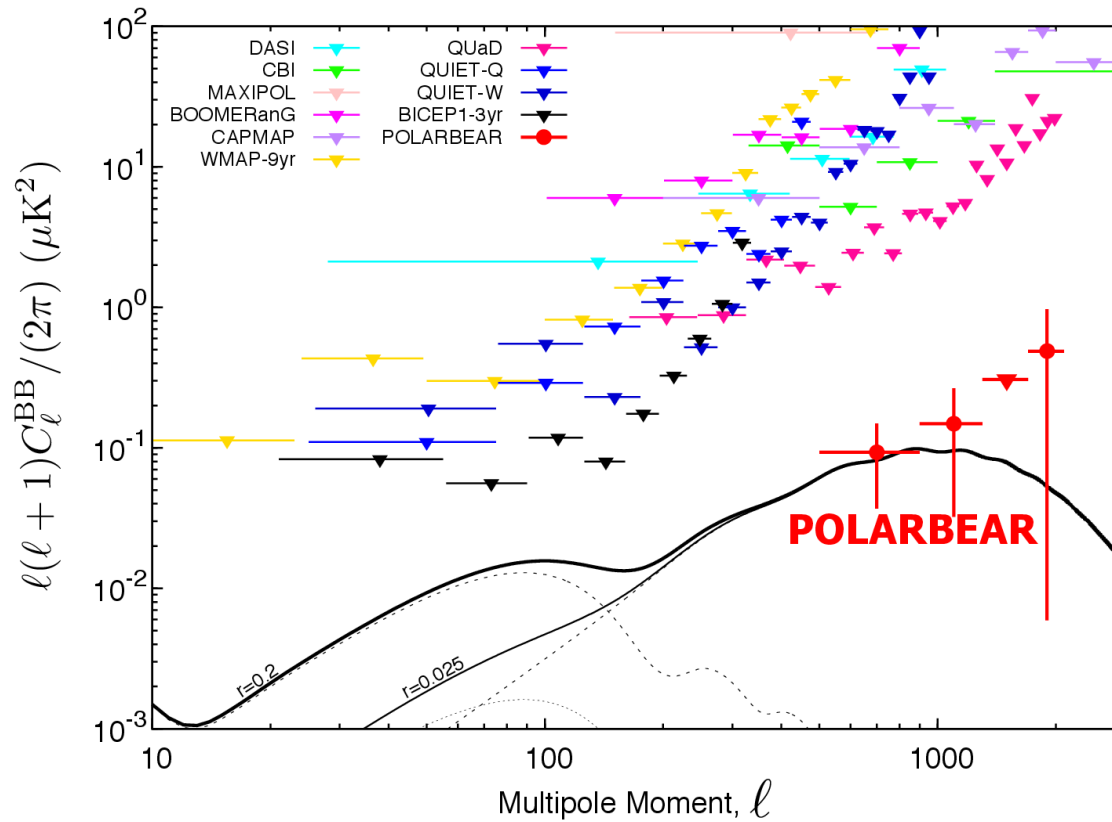


Status of observations

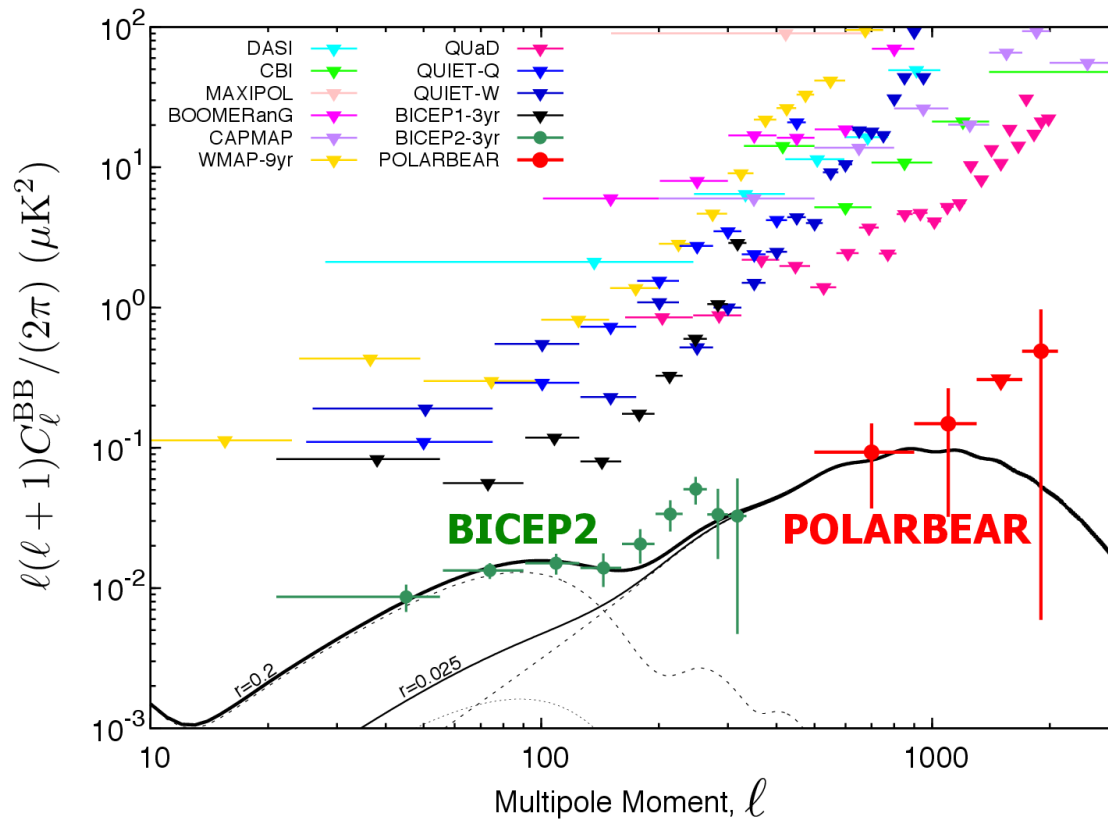
Early 2014



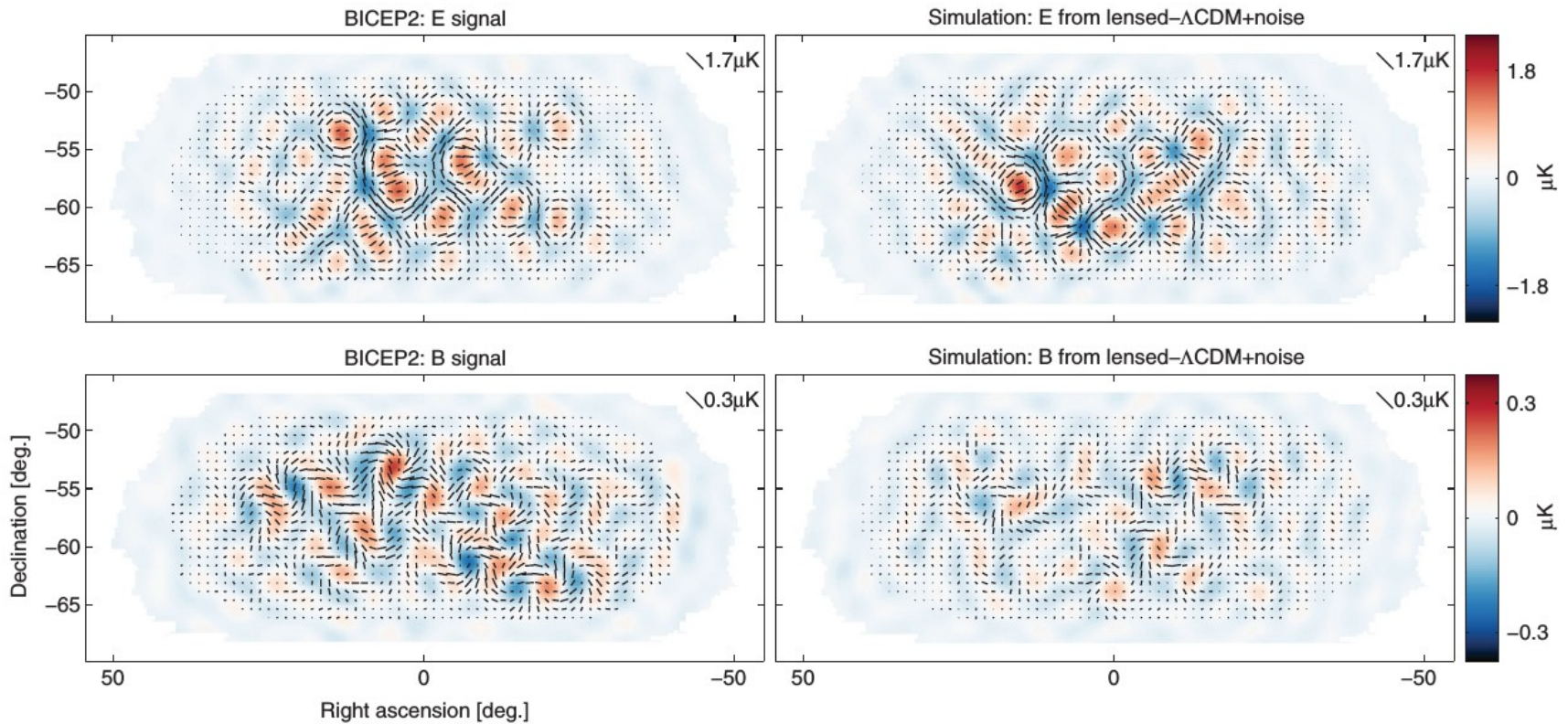
March 2014



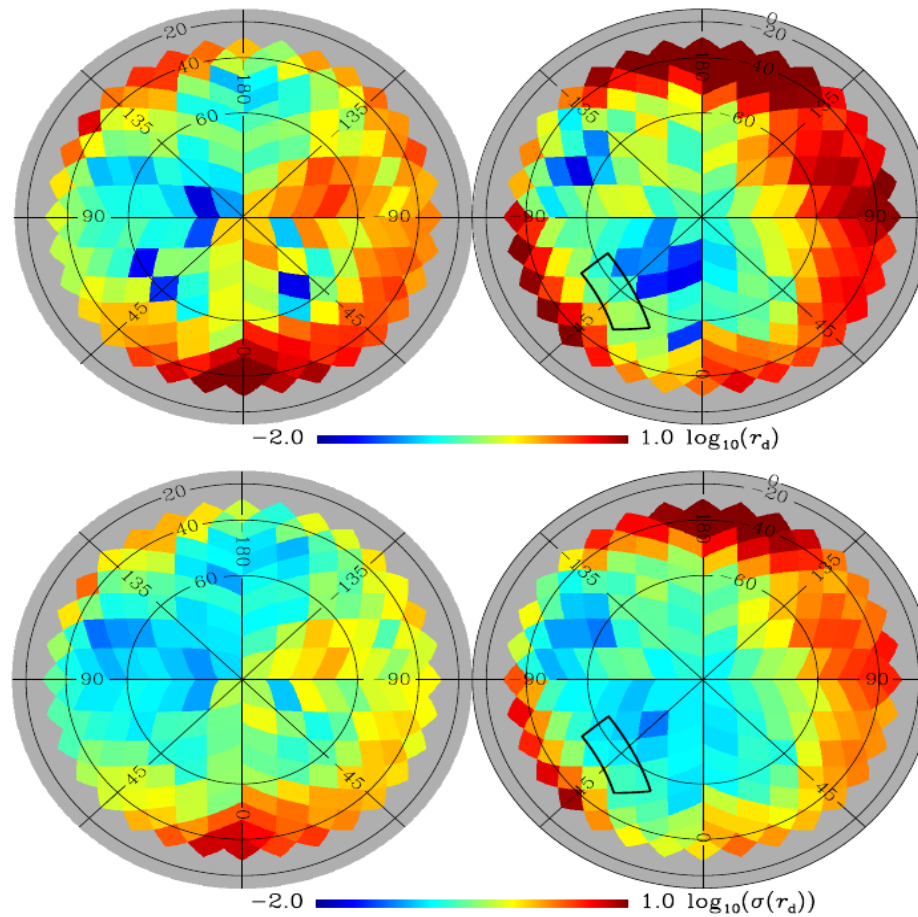
March 2014



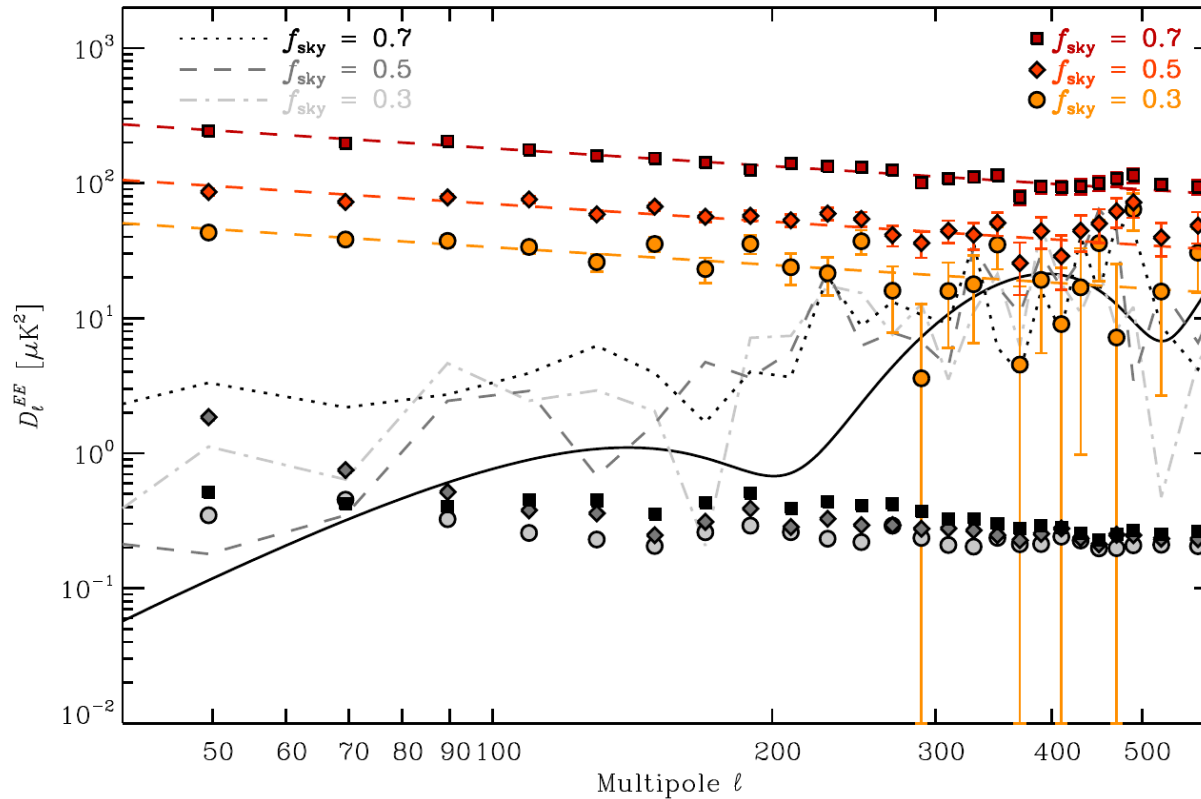
The B-modes at degree scale



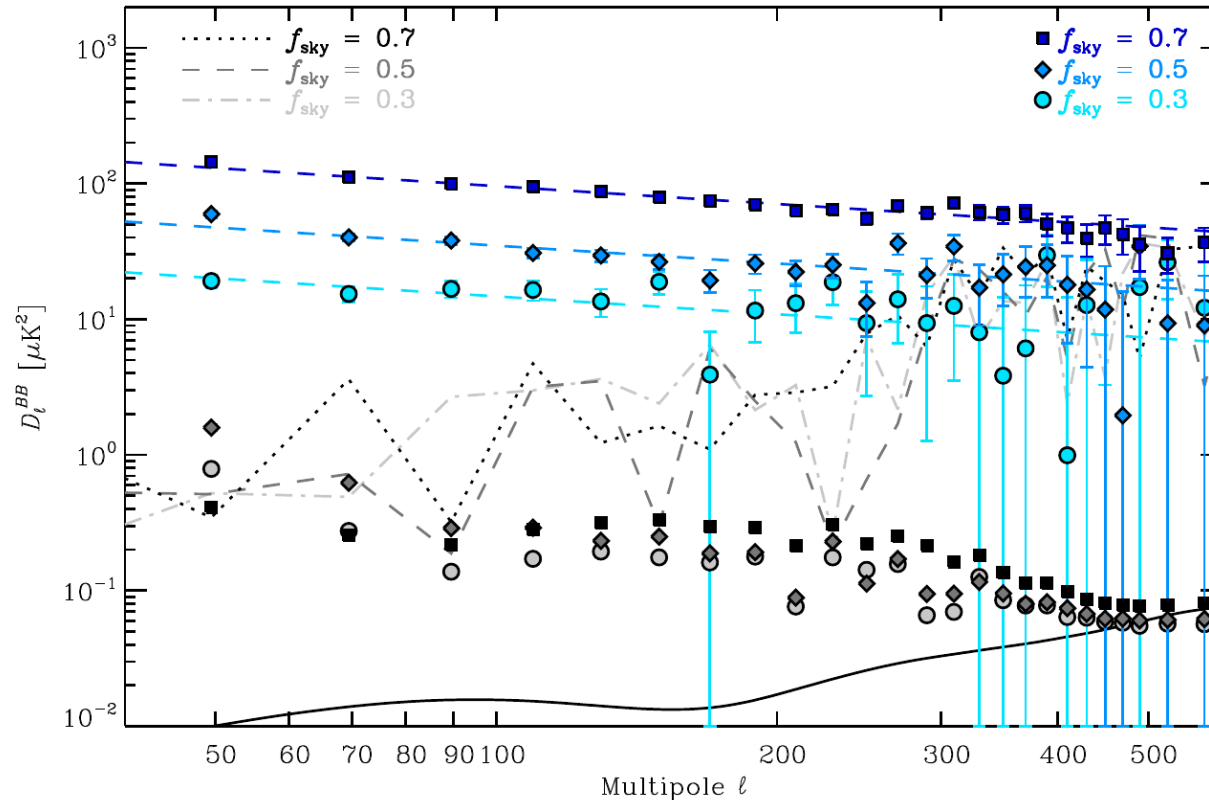
Planck observed dust polarization at high latitudes



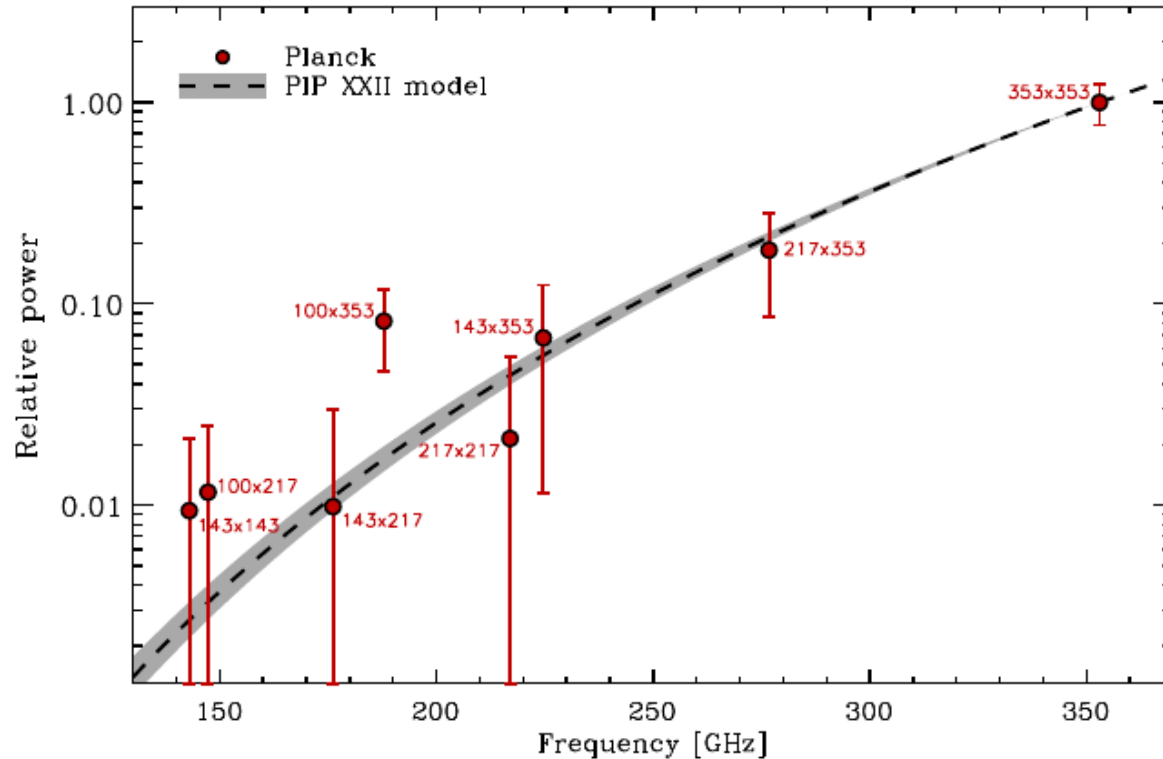
Planck observed dust polarization at high latitudes



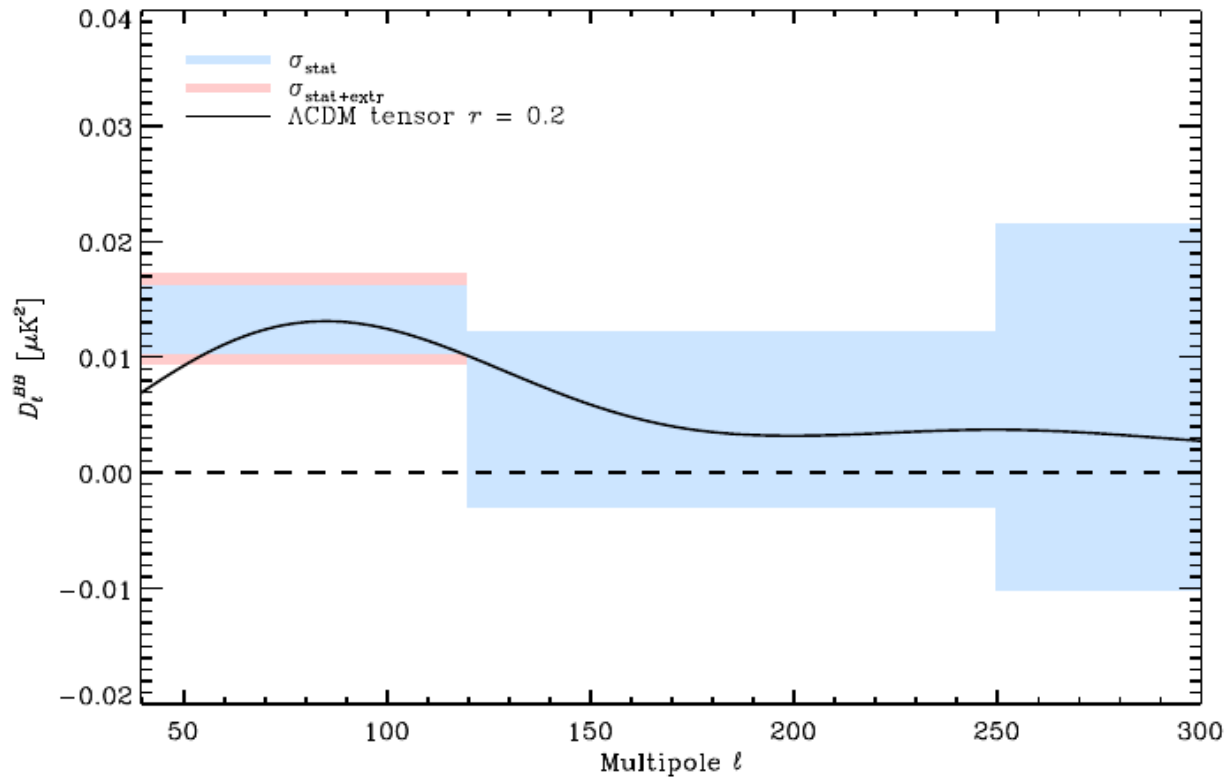
Planck observed dust polarization at high latitudes



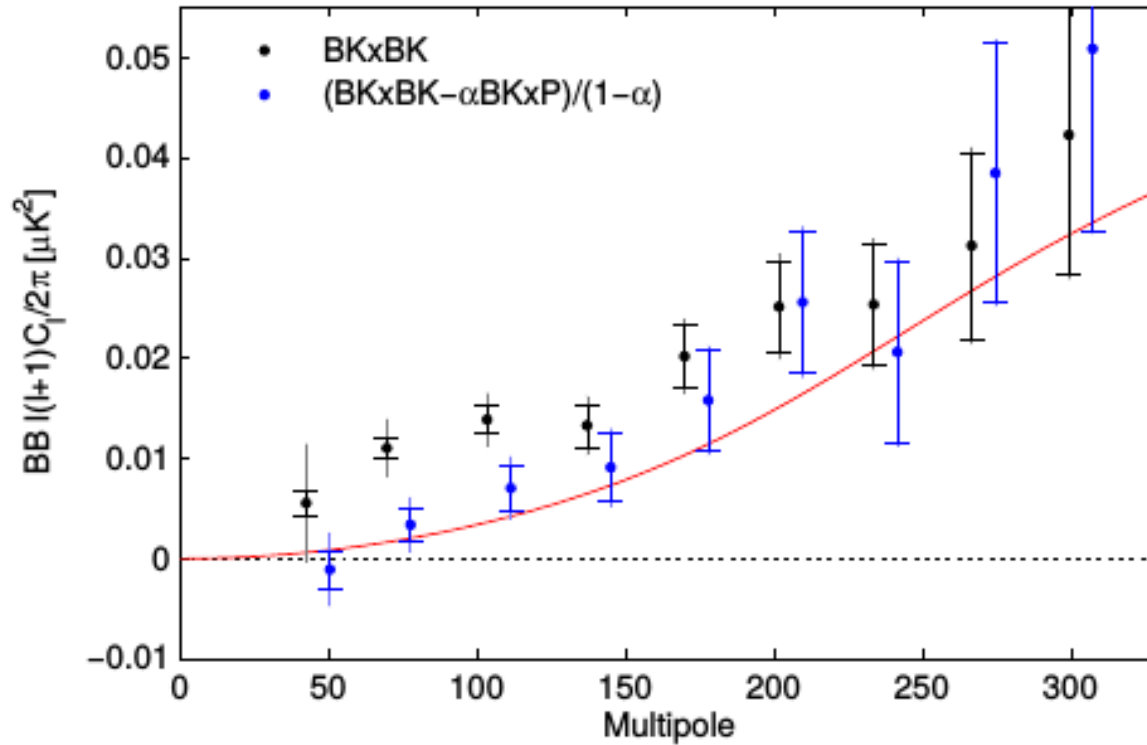
Planck observed dust polarization in the BICEP2 area



Planck observed dust polarization in the BICEP2 area



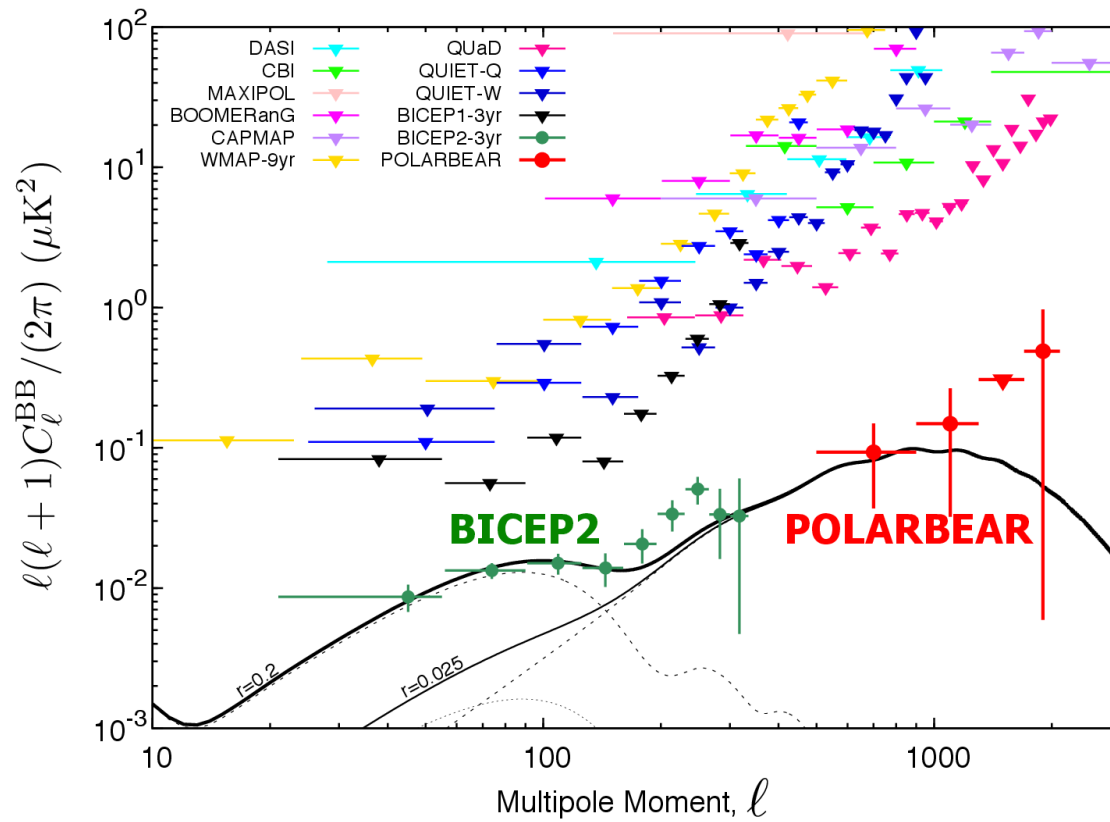
Planck × Bicep2 × KECK



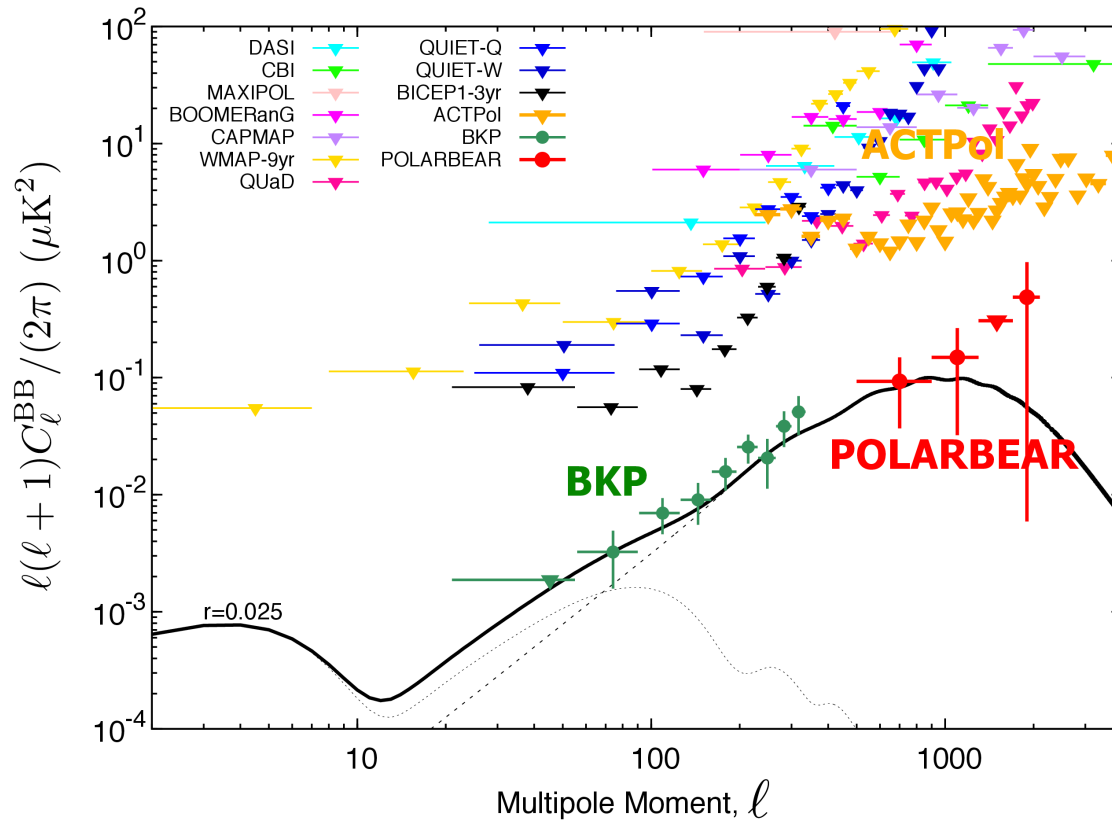
Planck × Bicep2 × KECK

$r < 0.12$ at 95% C.L.

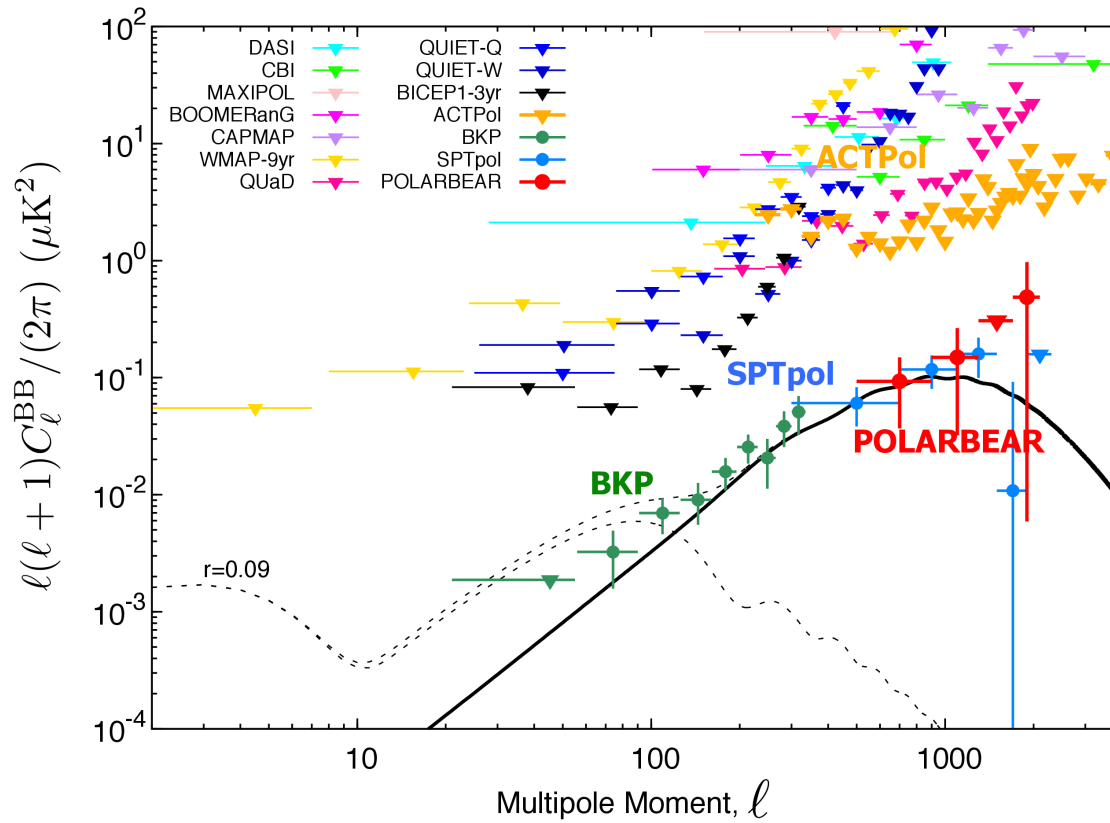
March 2014



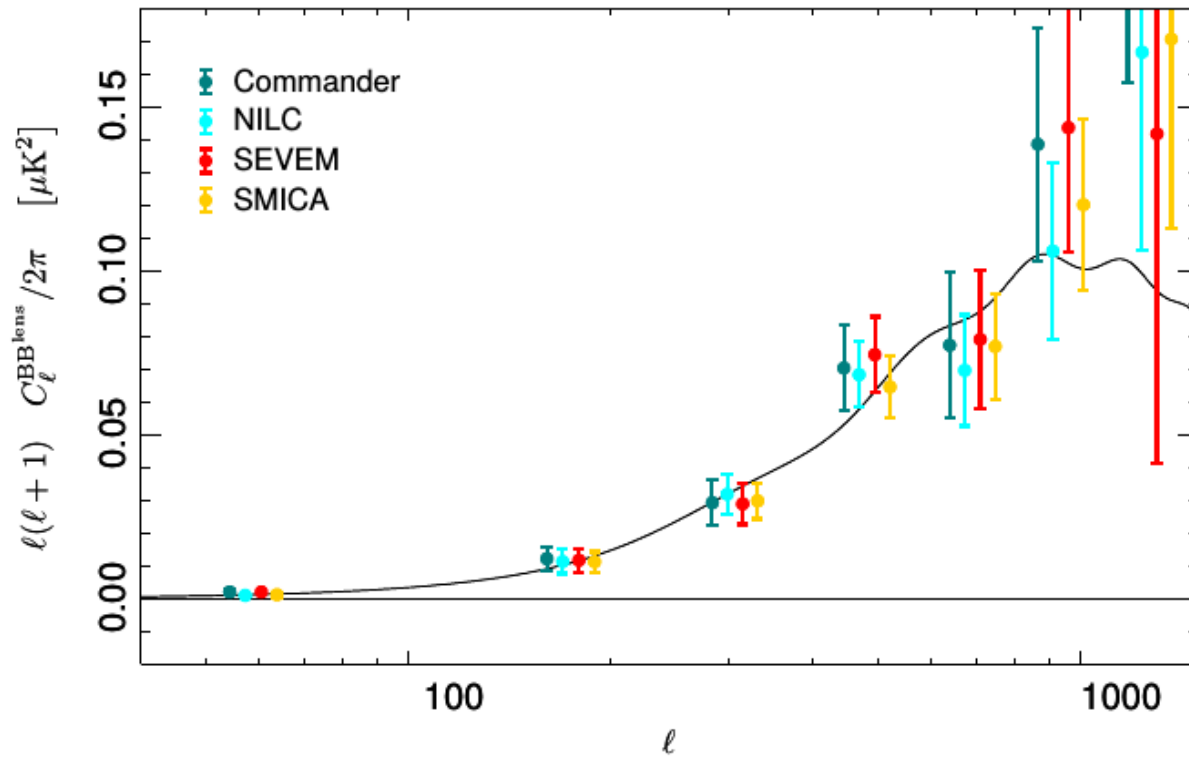
Now



Now



Now



Remarks

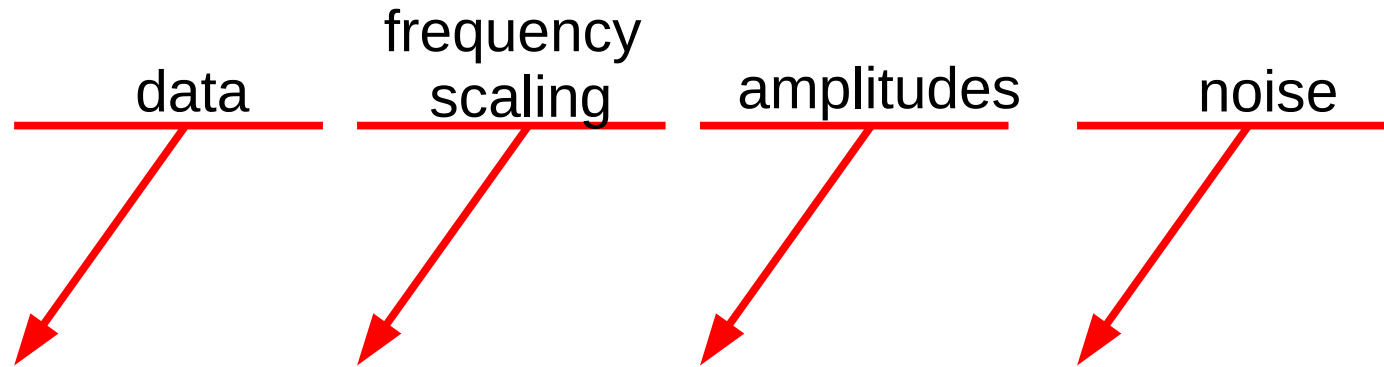
- The issue with diffuse foreground being comparable or dominant with respect to cosmologically interesting B-modes was guessed about a decade ago, and now confirmed by experiments
- Not only data, but data analysis progressed substantially to be able to include foreground cleaning into the data analysis pipeline
- The indication for operating experiments is clear: in addition to at least one CMB band, we need at least two bands per foreground (necessary but possibly not sufficient), with same angular resolution and sensitivity, in order to fit and marginalize foregrounds out

Component separation

Component separation

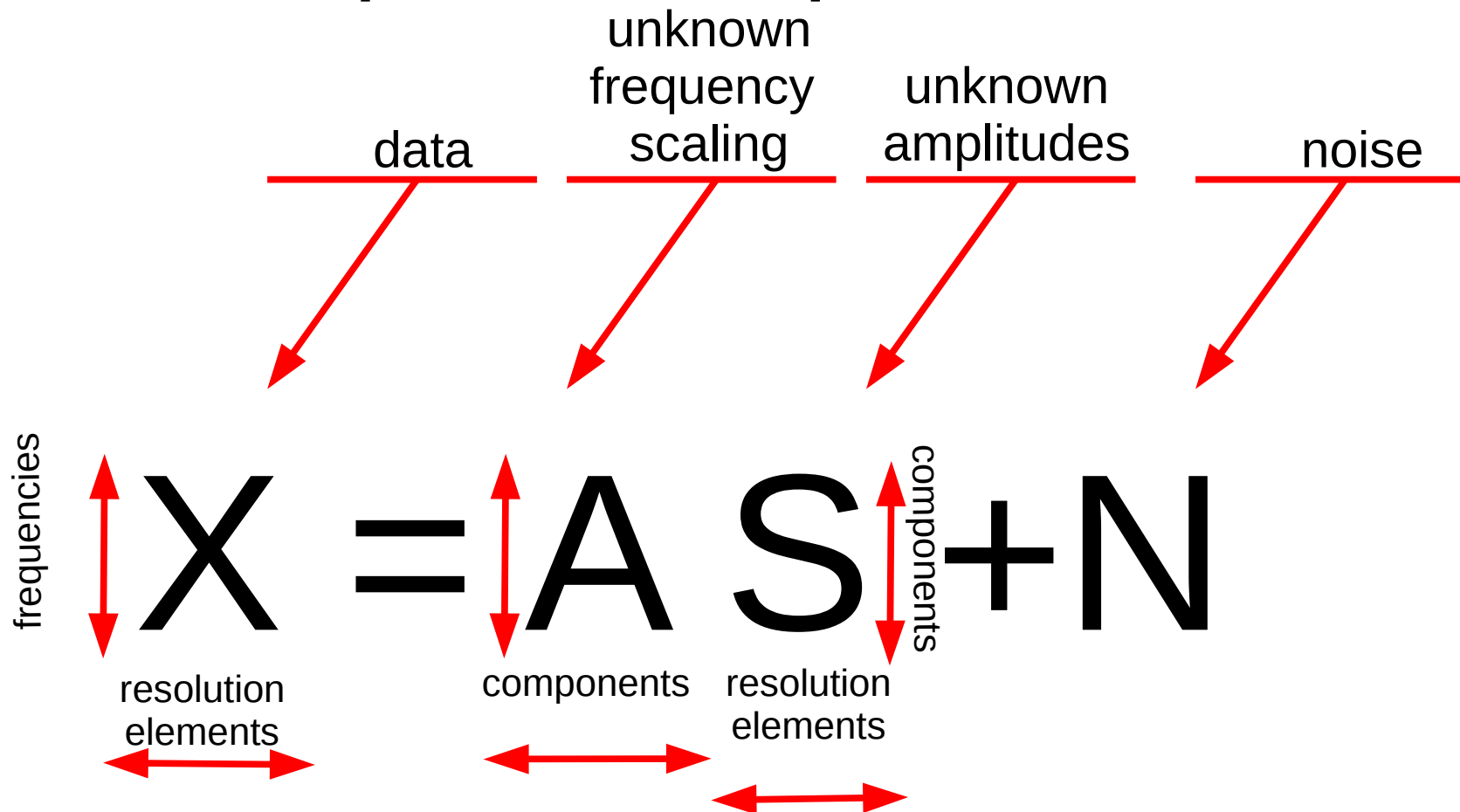
$$X = AS + N$$

Component separation



$$X = AS + N$$

Component separation



Component separation

- On foregrounds you...
 - Know nothing
 - Know something

Component separation

- Thus if you...
 - Know nothing, you
 - Look for minimum variance internal linear combination
 - Know something, you
 - Model foreground unknowns and fit

Component separation

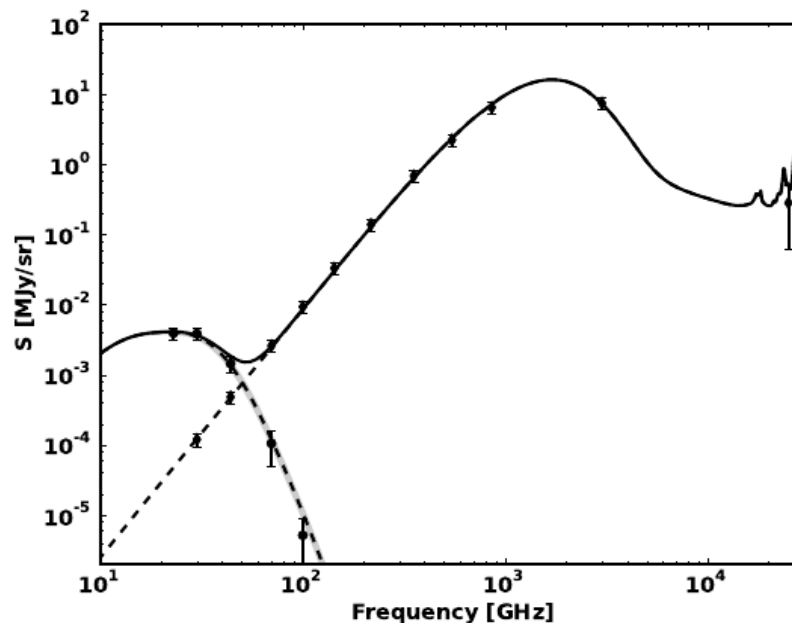
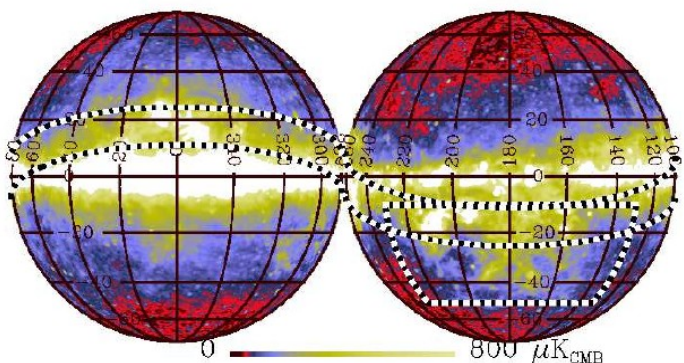
- If you know nothing, you
 - Look for minimum variance internal linear combination, constrained to scale as a black body:

$$\sum_i w_i X_i$$

$$\sum_i w_i = 1$$

Component separation

- If you know something, you
 - model and fit



Component separation

- Operating domains: you can choose to cast your minimum variance search, or your fit, in
 - Pixel domain
 - Harmonic domain
 - Intermediate (needlets, wavelets) domain

Component separation

- Thus if you...
 - Know nothing, you
 - Look for minimum variance internal linear combination
 - In the pixel domain
 - In the needlet domain
 - Know something, you
 - Model foreground unknowns and fit
 - In the pixel domain
 - In the needlet domain

Component separation

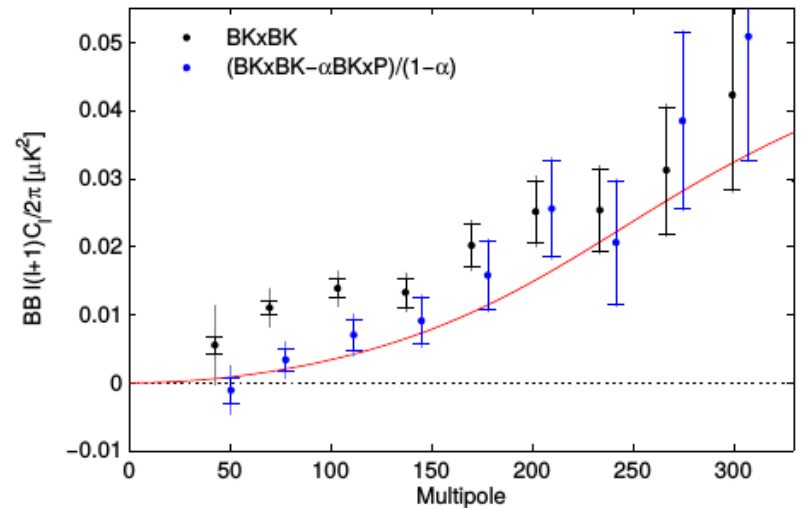
- Thus if you...
 - Know nothing, you
 - Look for minimum variance internal linear combination
 - In the pixel domain – SEVEM
 - In the needlet domain – NILC
 - Know something, you
 - Model foreground unknowns and fit
 - In the pixel domain – COMMANDER
 - In the needlet domain – SMICA

Component separation

- Thus if you...
 - Know nothing, you
 - Look for minimum variance internal linear combination
 - In the pixel domain – SEVEM (CMB only)
 - In the needlet domain – NILC (CMB only)
 - Know something, you
 - Model foreground unknowns and fit
 - In the pixel domain – COMMANDER (CMB and foregrounds)
 - In the needlet domain – SMICA (CMB and foregrounds)

Component separation for B-mode experiments

- Existing studies on simulations mostly based on parametric fitting
- Largely based on simulations till BKP15, which implements a template fitting in the harmonic domain
- Main driver for configurations of modern and future experiments aiming at the B-modes

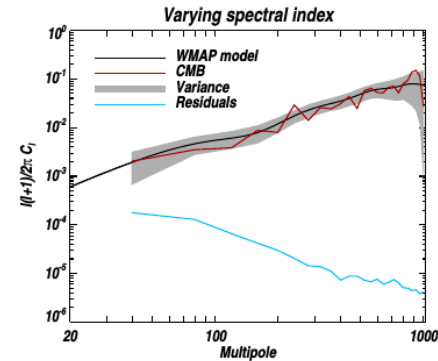
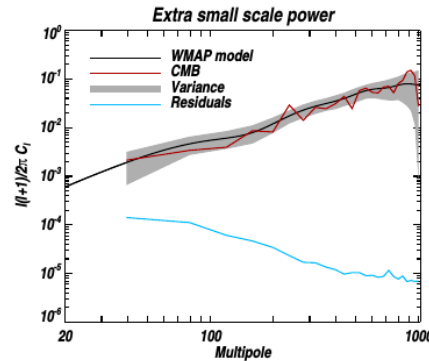
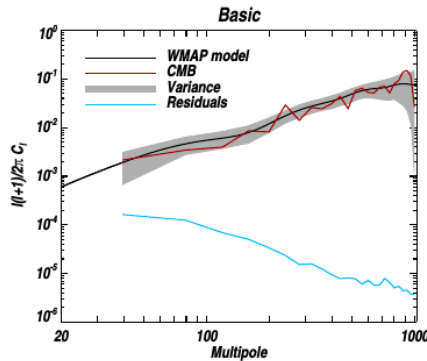
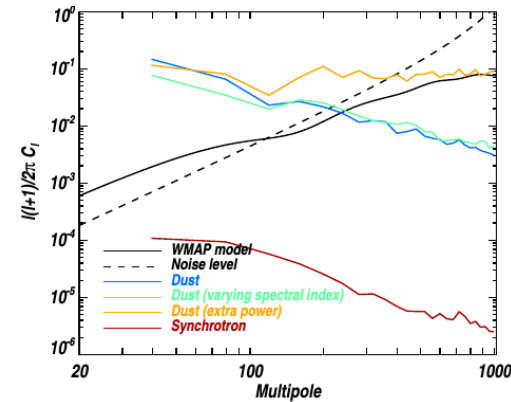


Component separation for B-mode experiments

- Casting in a maximum likelihood framework (Brandt et al. 1994, Eriksen et al. 2006, Stompor et al. 2009)
- Application to sub-orbital designs (Stivoli et al. 2010)
- Propagation to cosmological parameter estimation (Fantaye et al. 2011)
- Optimization scheme for sub-orbital designs proposed (Errard et al. 2011)
- Linearization and Fisher matrix for Quick Look Analysis (Errard & Stompor 2012)
- Check for effects on lensing reconstruction (Fantaye et al. 2012)

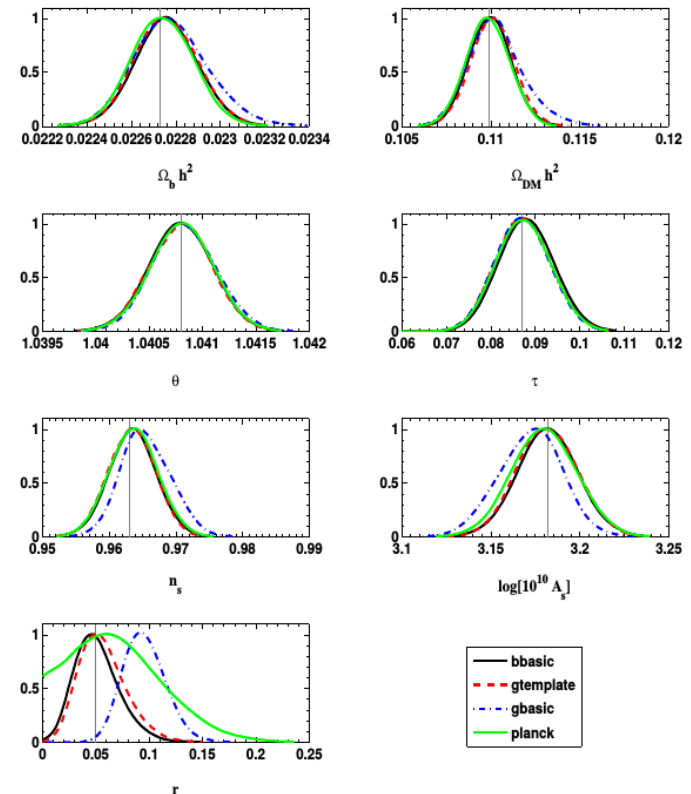
Balloon and ground-based setup analysis for B-foreground cleaning

- Considered designs: EBEX (150, 250, 410 GHz), PolarBear (90, 150, 220 GHz), targeting BICEP-like regions
- Dust removal successful for r of order percent for EBEX, possible bias for PolarBear due to unresolved residual synchrotron at 90 GHz

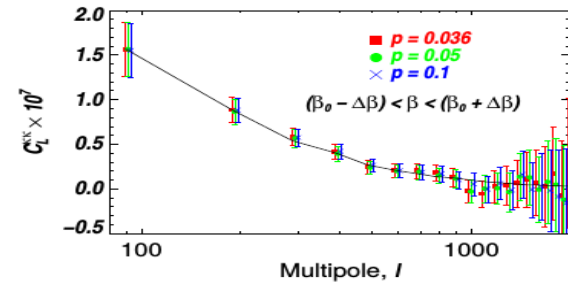
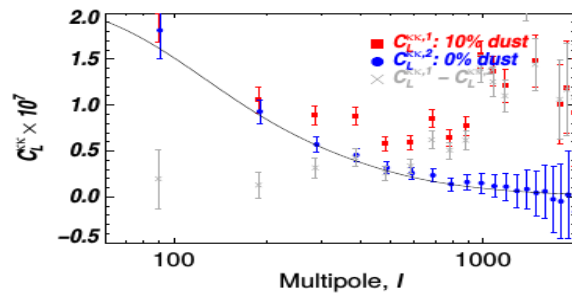
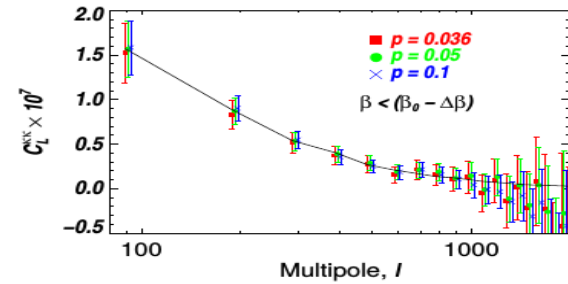
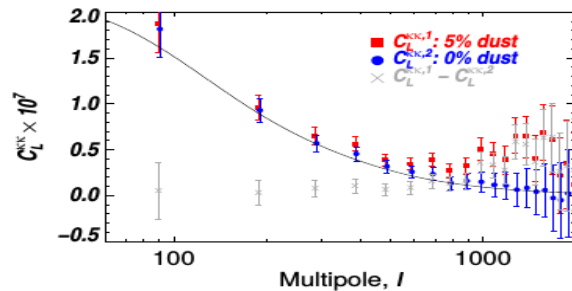
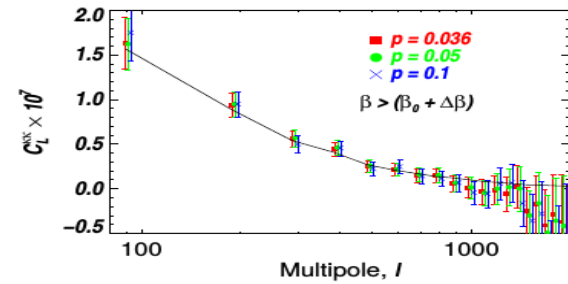
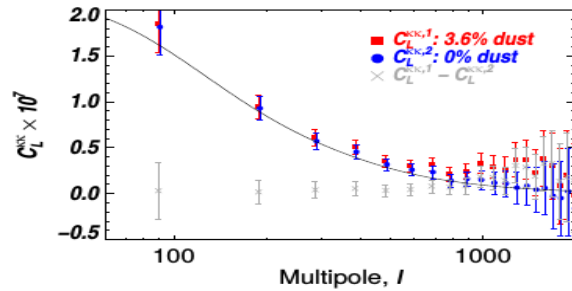


Balloon and ground-based setup analysis for B-foreground cleaning

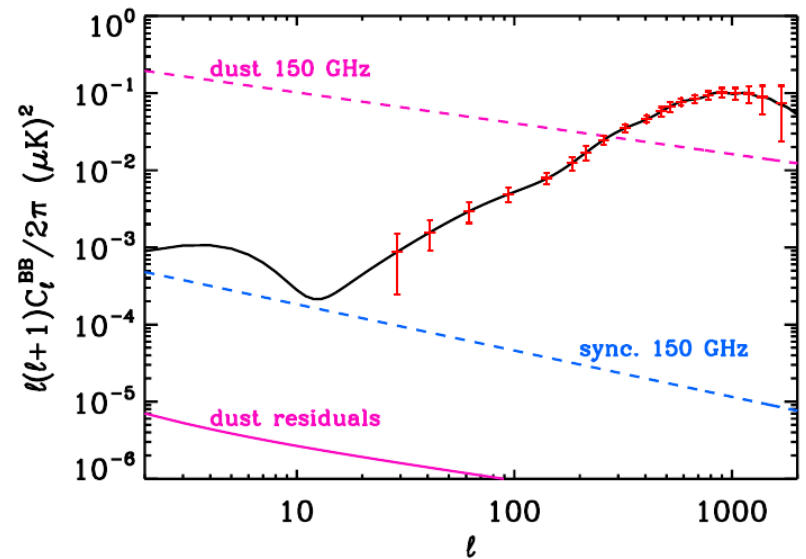
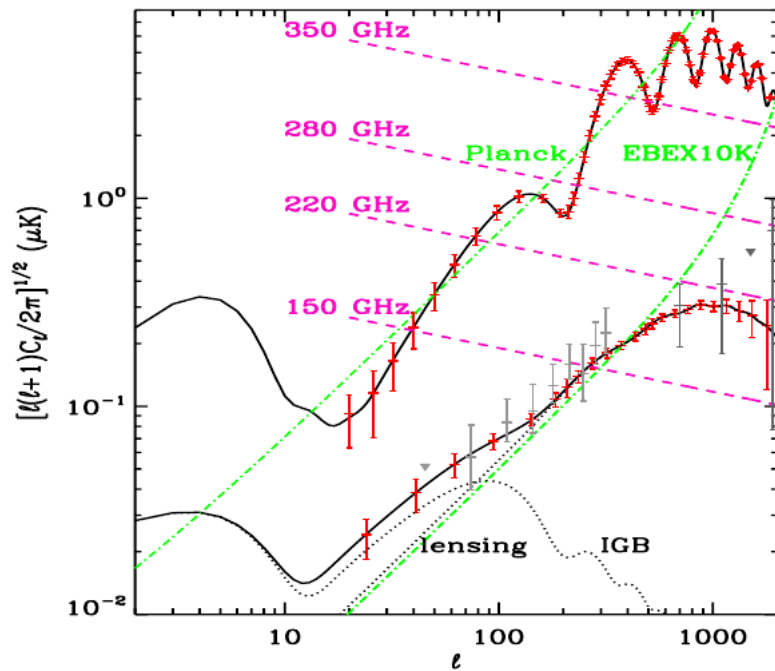
- Map-r end2end (no systematics) simulation responses:
 - no bias for 150, 250, 410 GHz setups, robust foreground monitor (EBEX, bbasic)
 - Possible bias from residual synchrotron in the foreground minimum (90 GHz) for ground measurements, alleviated if templates are available (PolarBear, gbasic)



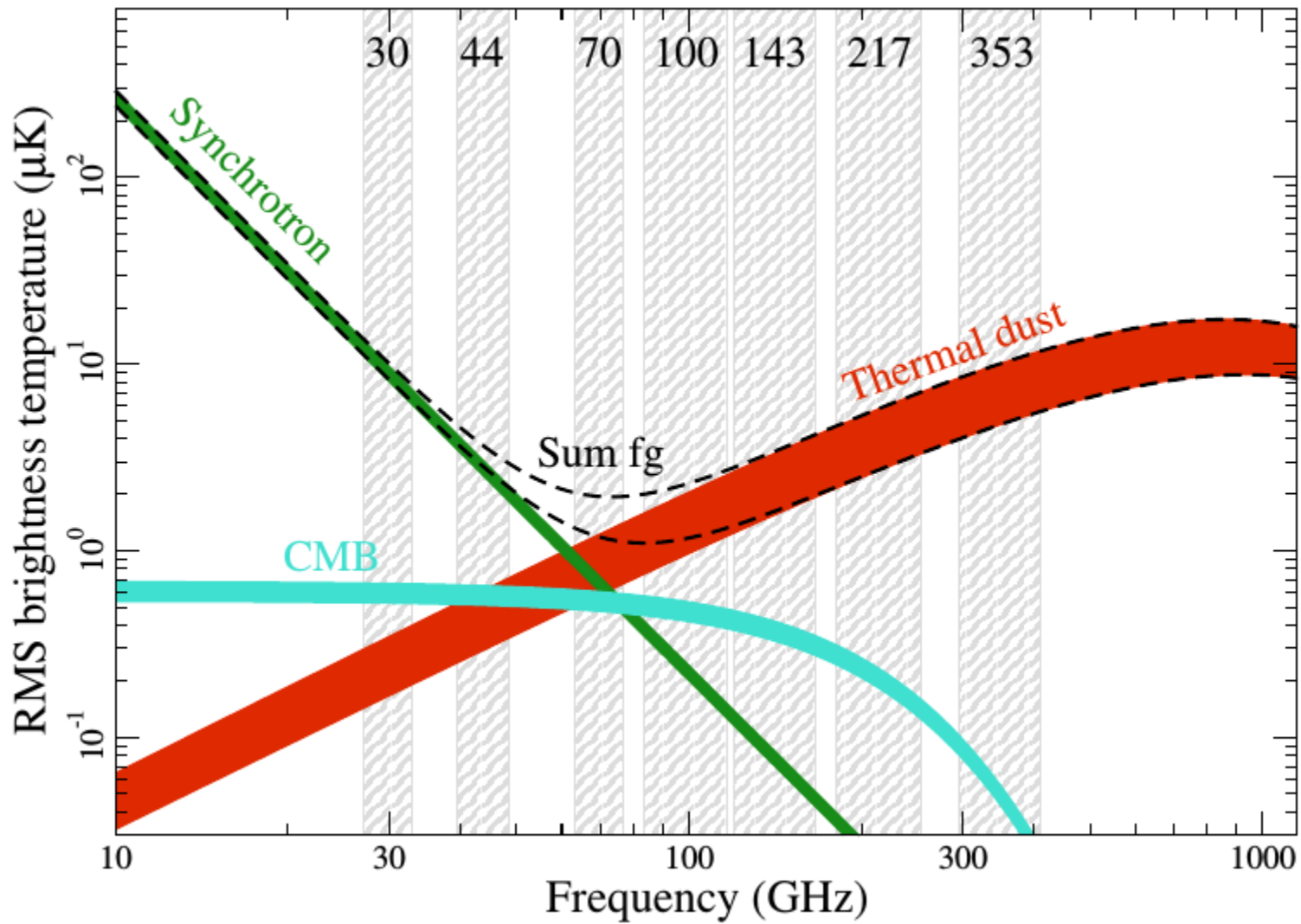
Dust residuals on lensing extraction

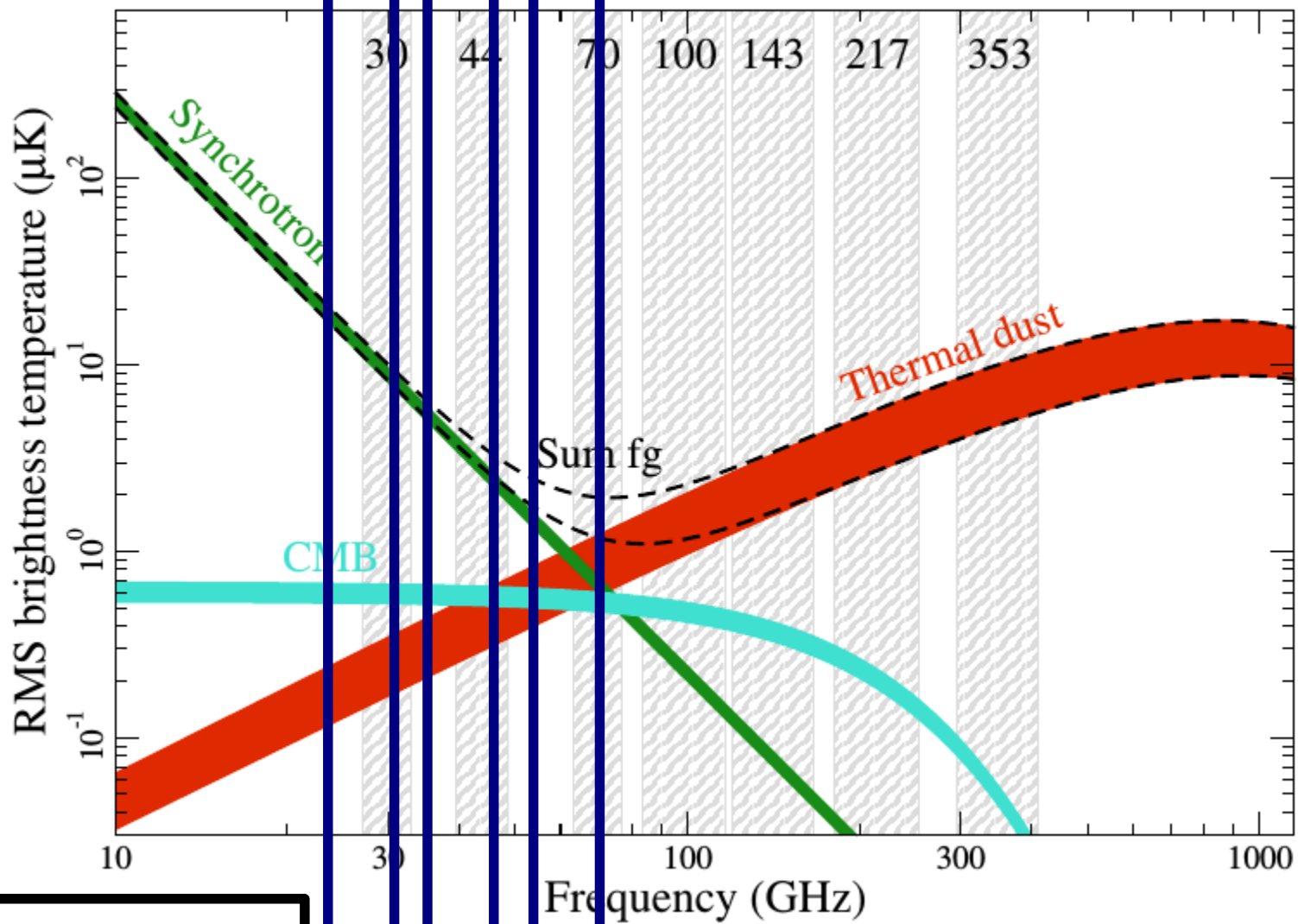


B-foreground cleaning driving experimental setups



Concluding
remarks





* **LFn:**
low frequency foreground band n

* **HFn:**
high frequency foreground band n

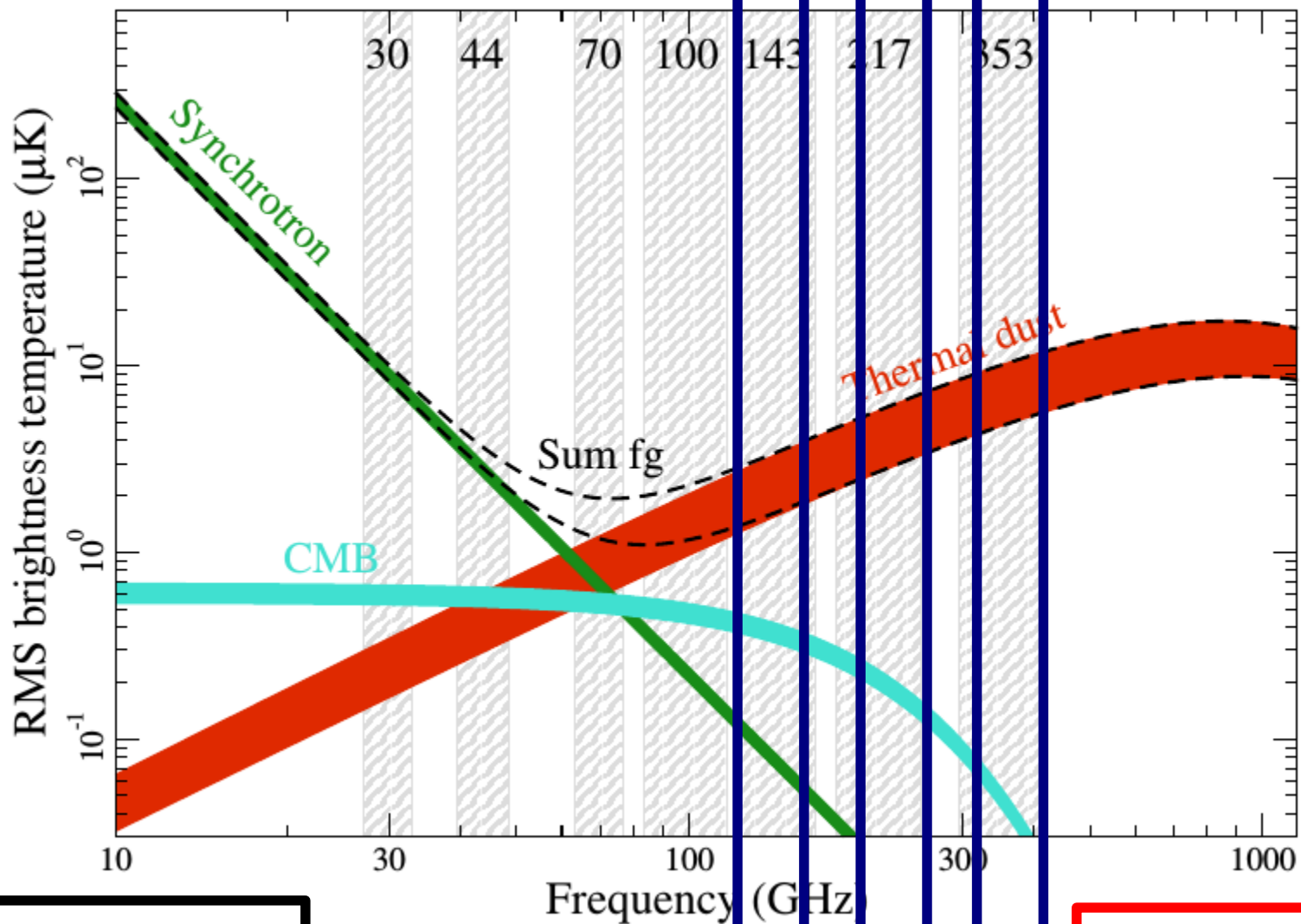
* **Angular resolution:**
All bands at few arcminutes FWHM

* **Sensitivity:**
All bands at few micro-K-arcminute

L
F
2

L
F
1

C
M
B



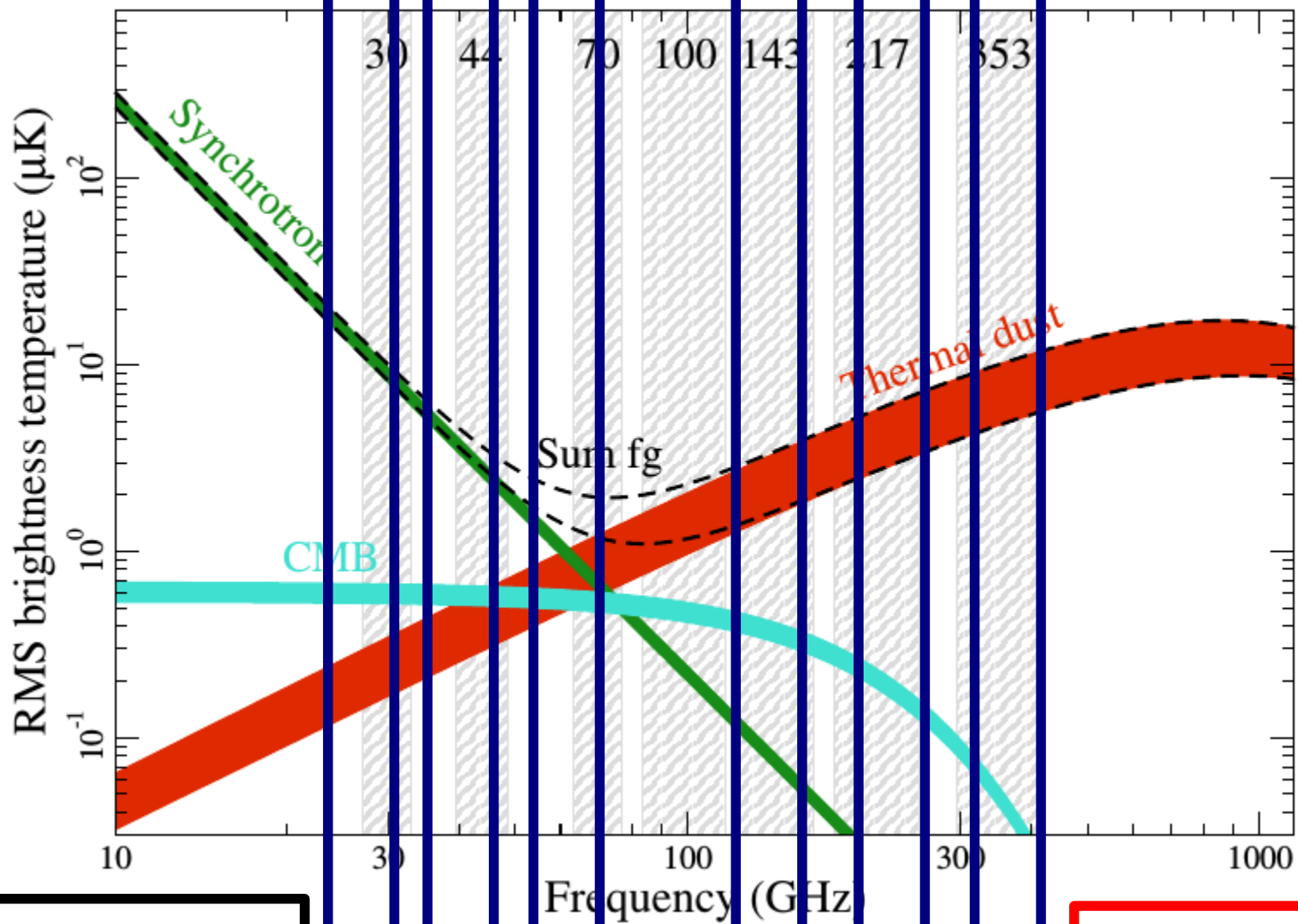
* **LFn:**
 low frequency foreground band n
 * **HFn:**
 high frequency foreground band n
 * **Angular resolution:**
 All bands at few arcminutes FWHM
 * **Sensitivity:**
 All bands at few micro-K-arcminute

C
M
B

H
F
1

H
F
2

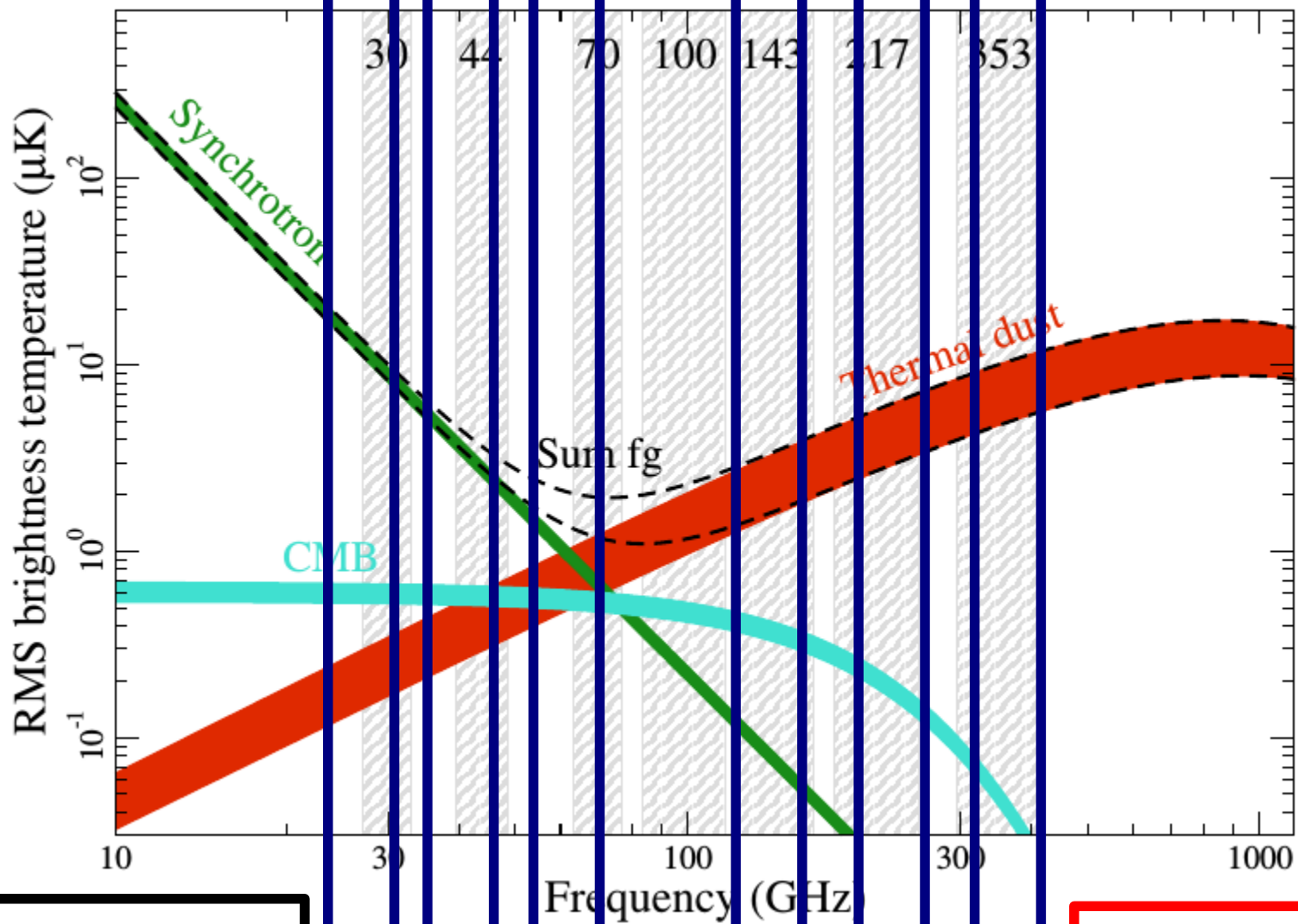
Considered for the
 configuration of sub-
 orbital probes
 (PolarBear, EBEX, ...)
 results \leq 2020



* **LFn:**
 low frequency foreground band n
 * **HFn:**
 high frequency foreground band n
 * **Angular resolution:**
 All bands at few arcminutes FWHM
 * **Sensitivity:**
 All bands at few micro-K-arcminute

L
F
2
 L
F
1
 C
M
B
 C
M
B
 H
F
1
 H
F
2

**Satellite/Combined
 sub-orbital Probes:**
 Litebird, PIXIE, S4,
 results > 2020

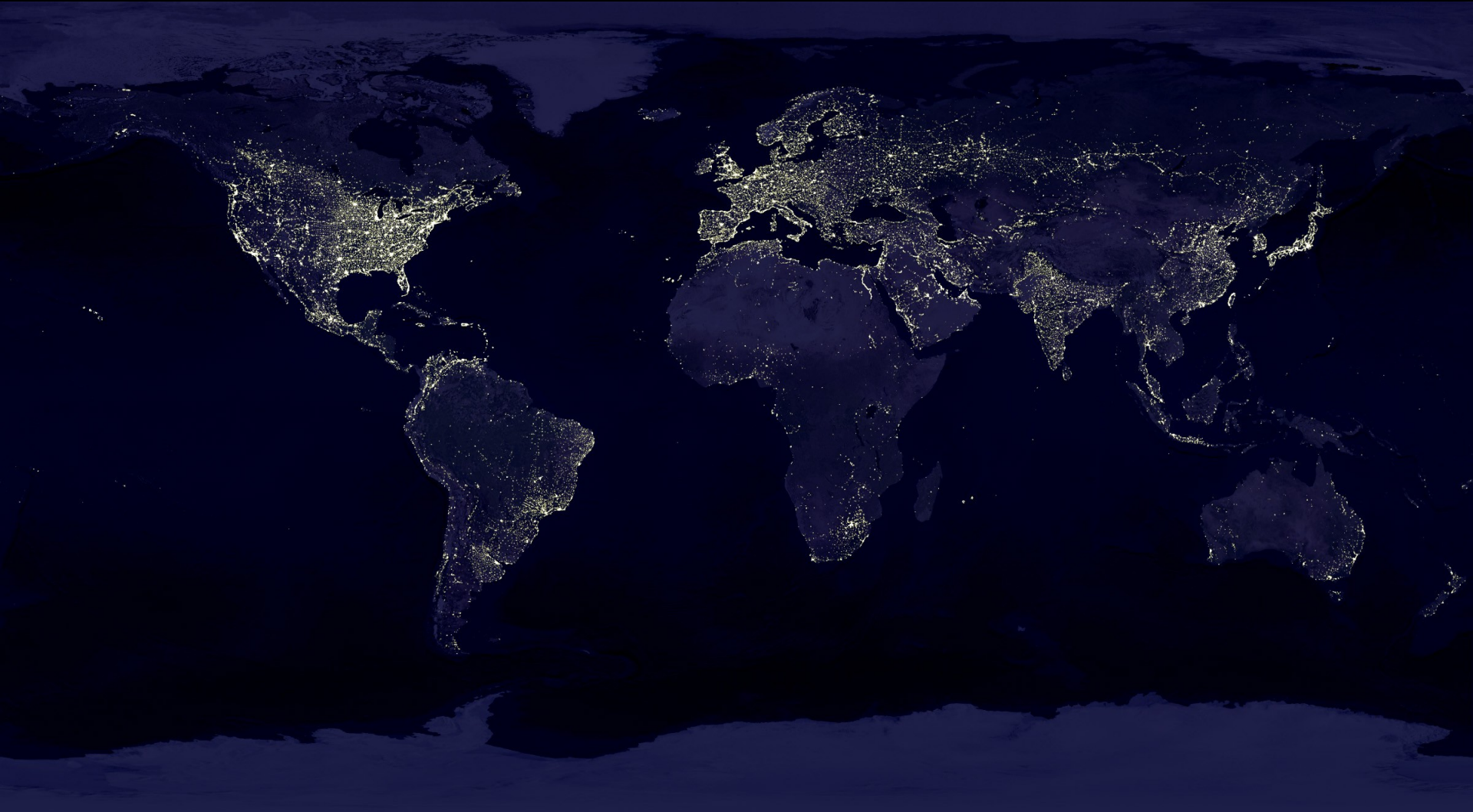


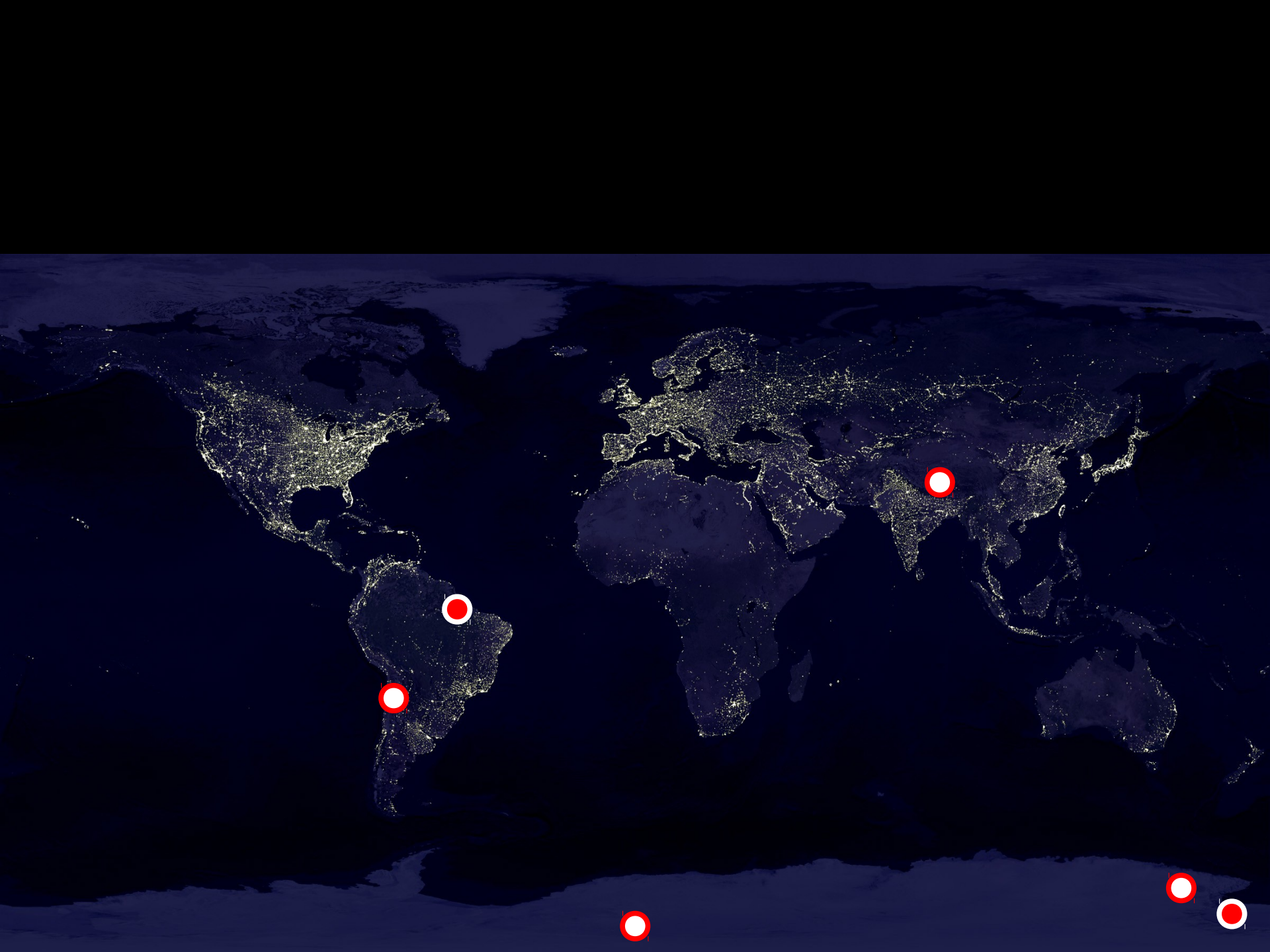
* **LFn:**
 low frequency foreground band n
 * **HFn:**
 high frequency foreground band n
 * **Angular resolution:**
 All bands at few arcminutes FWHM
 * **Sensitivity:**
 All bands at few micro-K-arcminute

LFn
 LFn
 CM
 CM
 HF
 HF

**Satellite/Combined
 sub-orbital Probes:**
 Litebird, PIXIE, S4,
 CORE+, results > 2020

Minimum detectable r: $\text{few} \times 10^{-3}$





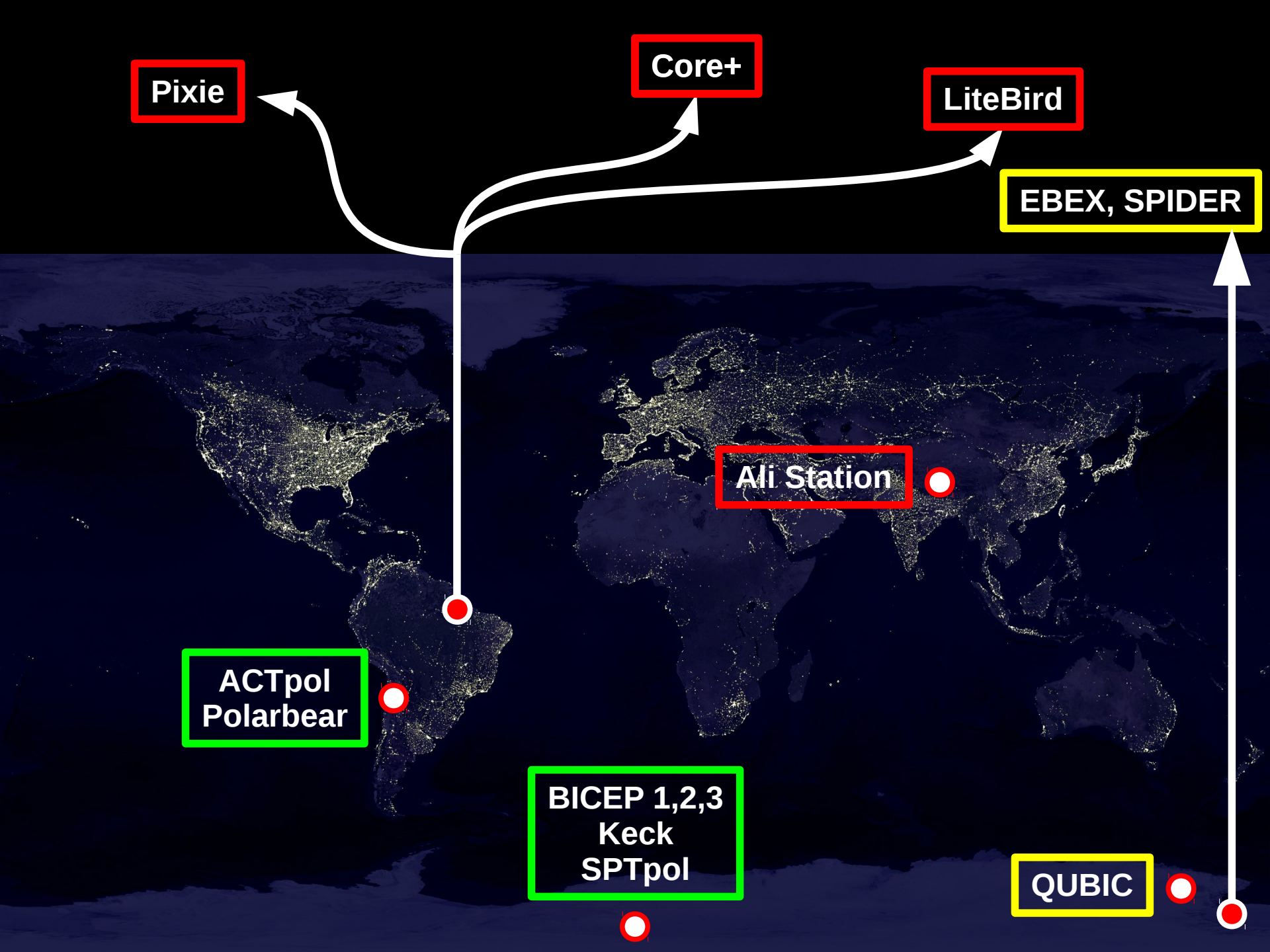


ACTpol
Polarbear

Ali Station

BICEP 1,2,3
Keck
SPTpol

QUBIC



Pixie

Core+

LiteBird

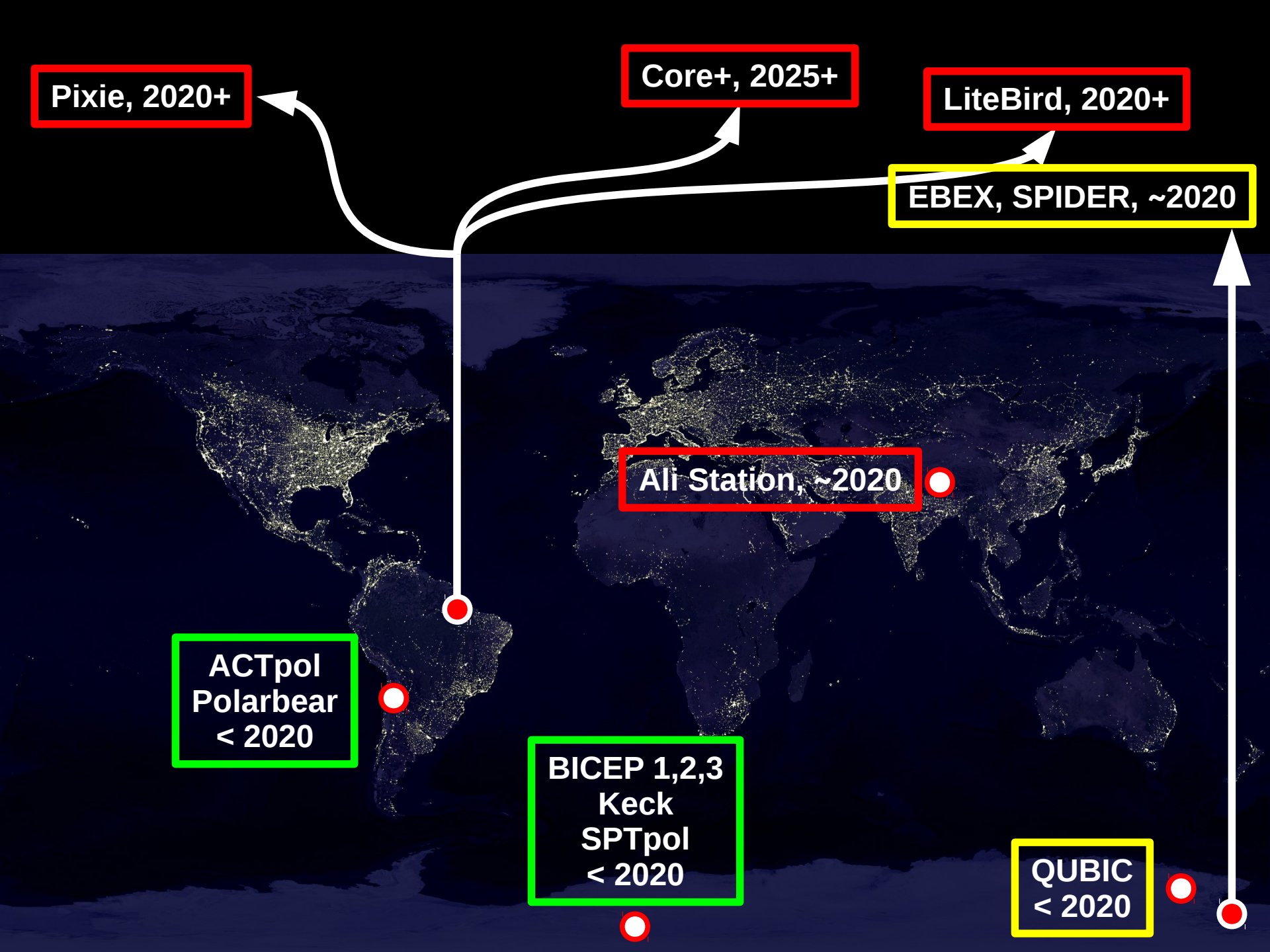
EBEX, SPIDER

Ali Station

ACTpol
Polarbear

BICEP 1,2,3
Keck
SPTpol

QUBIC



Pixie, 2020+

Core+, 2025+

LiteBird, 2020+

EBEX, SPIDER, ~2020

Ali Station, ~2020

ACTpol
Polarbear
< 2020

BICEP 1,2,3
Keck
SPTpol
< 2020

QUBIC
< 2020

Backup slides

CORE+ configuration

| channel GHz | beam arcmin | N_{det} | ΔT $\mu K \cdot \text{arcmin}$ | ΔP $\mu K \cdot \text{arcmin}$ | ΔI kJy/sr.arcmin | $\Delta y \times 10^6$ $y_{\text{SZ}} \cdot \text{arcmin}$ | PS flux (5σ) mJy |
|----------------|----------------|------------------|---|---|-----------------------------|---|------------------------------|
| 60 | 14 | 28 | 11.3 | 16 | 1.14 | -2.3 | 6 |
| 70 | 12 | 30 | 10.5 | 14.9 | 1.4 | -2.2 | 6.3 |
| 80 | 10.5 | 38 | 9.1 | 12.9 | 1.53 | -2.0 | 6 |
| 90 | 9.33 | 72 | 6.5 | 9.2 | 1.32 | -1.5 | 4.6 |
| 100 | 8.4 | 84 | 6.0 | 8.5 | 1.43 | -1.5 | 4.5 |
| 115 | 7.3 | 124 | 5.0 | 7.0 | 1.45 | -1.3 | 4 |
| 130 | 6.46 | 180 | 4.2 | 5.9 | 1.43 | -1.3 | 3.5 |
| 145 | 5.79 | 264 | 3.6 | 5.0 | 1.37 | -1.3 | 3 |
| 160 | 5.25 | 254 | 3.8 | 5.4 | 1.6 | -1.7 | 3.1 |
| 175 | 4.8 | 290 | 3.8 | 5.3 | 1.69 | -2.2 | 3.0 |
| 195 | 4.31 | 346 | 3.8 | 5.3 | 1.79 | -4.1 | 2.9 |
| 220 | 3.82 | 200 | 5.8 | 8.1 | 2.78 | - | 4.0 |
| 255 | 3.29 | 140 | 8.9 | 12.6 | 4.11 | 5.5 | 5.1 |
| 295 | 2.85 | 60 | 19.4 | 27.4 | 7.84 | 5.7 | 8.4 |
| 340 | 2.47 | 60 | 30.9 | 43.7 | 9.91 | 5.6 | 9.2 |
| 390 | 2.15 | 60 | 55.0 | 77.8 | 12.63 | 7.0 | 10.2 |
| 450 | 1.87 | 60 | 116.6 | 164.8 | 16.48 | 10.9 | 11.5 |
| 520 | 1.62 | 60 | 295.7 | 418.2 | 21.71 | 21.0 | 13.2 |
| 600 | 1.4 | 60 | 899.7 | 1272.4 | 28.61 | 50.3 | 15.0 |

LiteBird configuration

| Band GHz | Beam [†] [arcmin] | NET [$\mu K \sqrt{s}$] | Pixel # per wafer | Wafer # | Bolometer # | NETarr [$\mu K \sqrt{s}$] | Sensitivity [$\mu K \text{arcmin}$] |
|-------------|-------------------------------|-----------------------------|----------------------|---------|-------------|--------------------------------|--|
| 60 | 75 | 99 | 19 | 8 | 304 | 5.7 | 10.3 |
| 78 | 58 | 62 | 19 | 8 | 304 | 3.6 | 6.5 |
| 100 | 45 | 45 | 19 | 8 | 304 | 2.6 | 4.7 |
| 140 | 32 | 40 | 37 | 5 | 370 | 2.1 | 3.7 |
| 195 | 24 | 33 | 37 | 5 | 370 | 1.7 | 3.1 |
| 280 | 16 | 40 | 37 | 5 | 370 | 2.1 | 3.8 |

Planck observed dust polarization at high latitudes

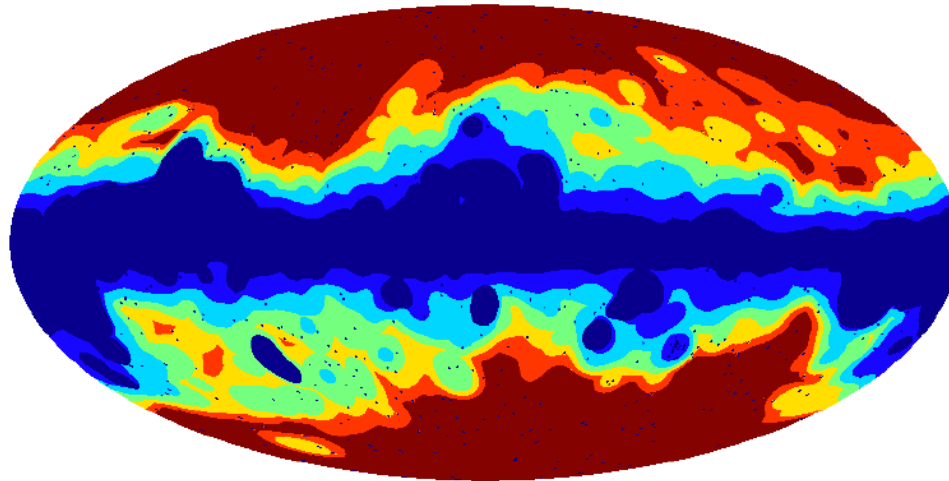


Fig. 1: Masks and complementary selected large regions that retain fractional coverage of the sky f_{sky} from 0.8 to 0.3 (see details in Sect. 3.3.1). The darkest blue is the CO mask, whose complement is a selected region with $f_{\text{sky}} = 0.8$. In increments of $f_{\text{sky}} = 0.1$, the retained regions can be identified by the colours dark red (0.3) to dark blue (0.8), inclusively. Also shown is the (unapodized) point source mask used.

Planck observed dust polarization in the BICEP2 area

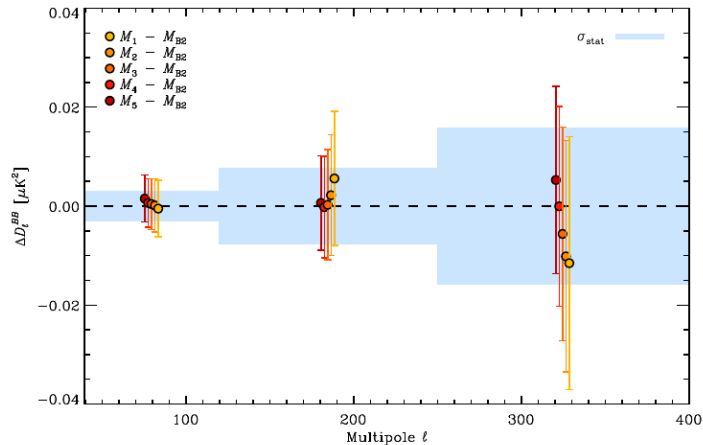


Fig. C.2: *Planck* 353 GHz \mathcal{D}_ℓ^{BB} angular power spectrum differences extrapolated to 150 GHz, determined from the spectra computed on the M_{1-5} regions presented in Appendix C.2 and the spectrum computed on M_{B2} . \mathcal{D}_ℓ^{BB} difference values for the five regions are displayed using colours from yellow (for M_1) to dark red (for M_5). As in Fig. 9, the blue boxes represent the statistical uncertainties from noise associated with the M_{B2} spectrum. They are centred on zero, since we compute spectrum differences here.

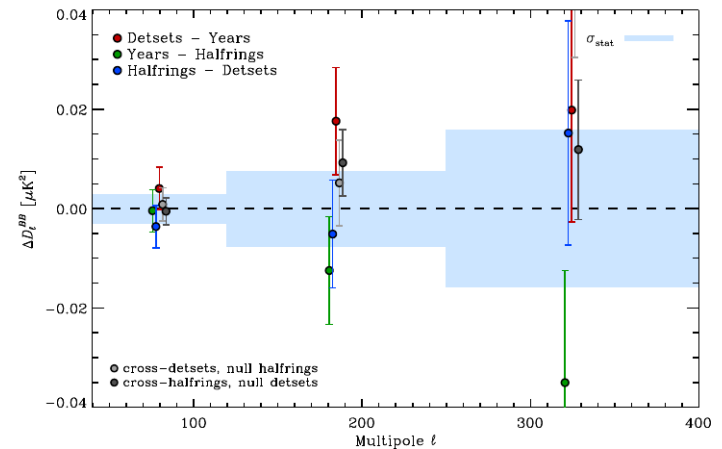


Fig. C.3: *Planck* 353 GHz \mathcal{D}_ℓ^{BB} angular power spectrum differences extrapolated to 150 GHz, computed from the following cross-spectra differences: DetSets minus Years (red circles); Years minus HalfRings (green circles); and HalfRings minus DetSets (blue circles). We also show the null test performed using the cross-DetSets spectra of the HalfRing half-differences (light grey circles) and the cross-HalfRings of the DetSet half-differences (dark grey circles) at 353 GHz. As in Fig. 9, the blue boxes represent the statistical uncertainties from noise; these are centred on zero, since we do not expect any signal for these null tests.

The Planck polarisation at 353 GHz: the BICEP2 area

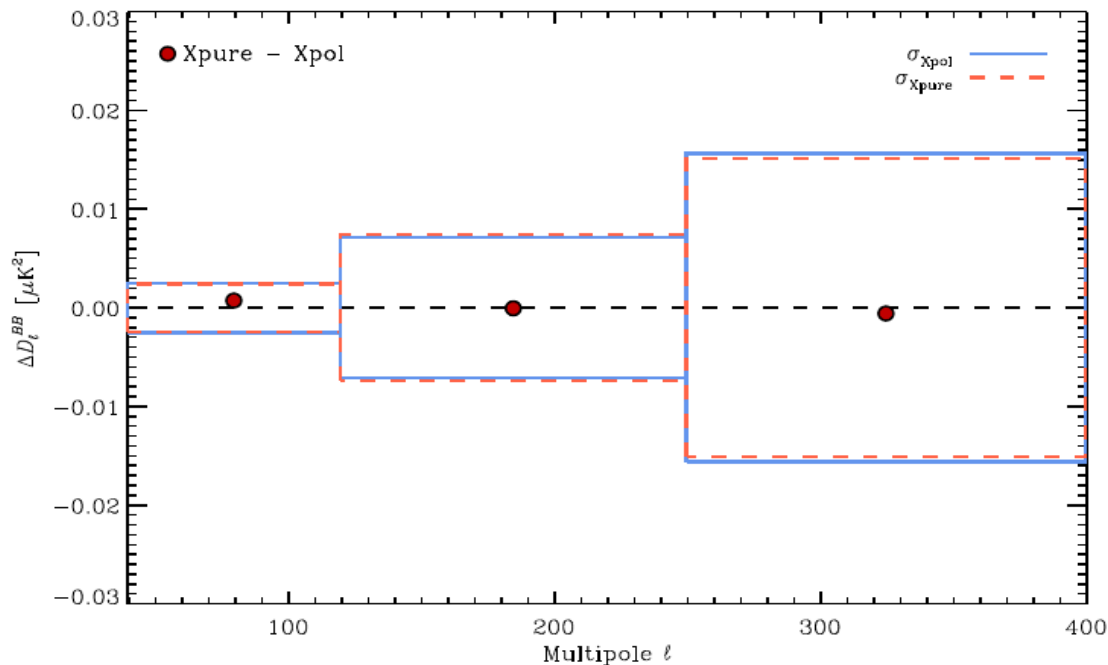


Fig. C.1: X_{pol} minus X_{pure} *Planck* 353 GHz \mathcal{D}_ℓ^{BB} angular power spectrum differences extrapolated to 150 GHz, computed from the cross-DetSets on M_{B2} (red circles). The blue boxes represent the $\pm 1\sigma$ errors computed using X_{pol} from the data on M_{B2} , while the dashed-orange boxes are the X_{pure} $\pm 1\sigma$ errors coming from Monte Carlo simulations of *Planck* noise.

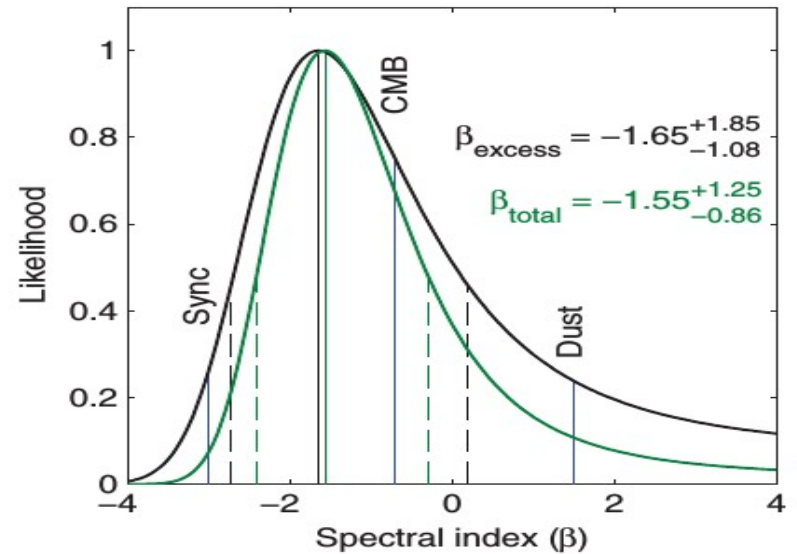
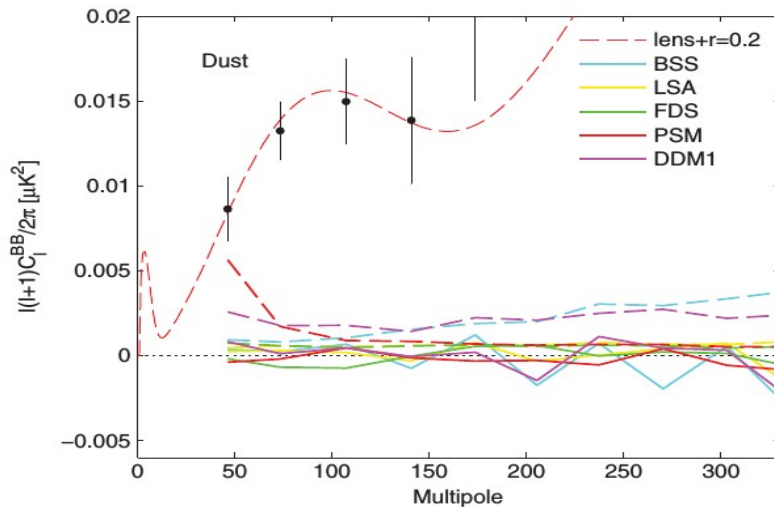
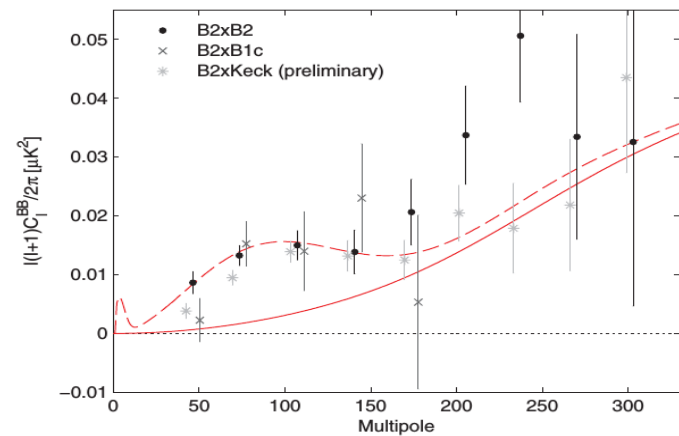
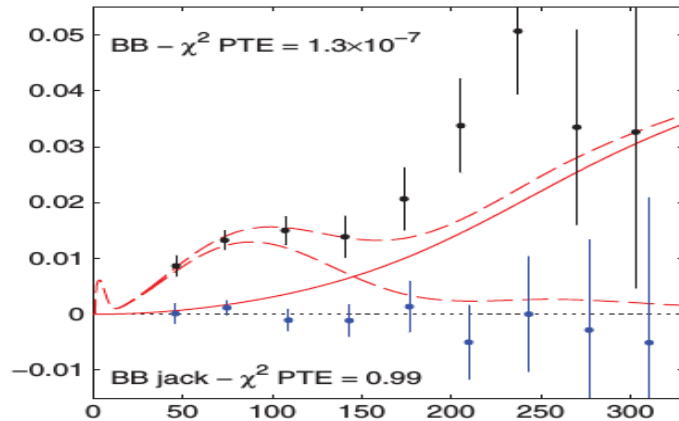
Foreground model building

- Start from total intensity measurements, if available
- Get polarized intensity by imposing a constant polarization fraction
- Construct a pattern for the polarization angle, starting from large scale measurements, adding by hand small scale power according to various recipes
- Assume the same spectral variation for total intensity and polarization
- Check everything with observations when available

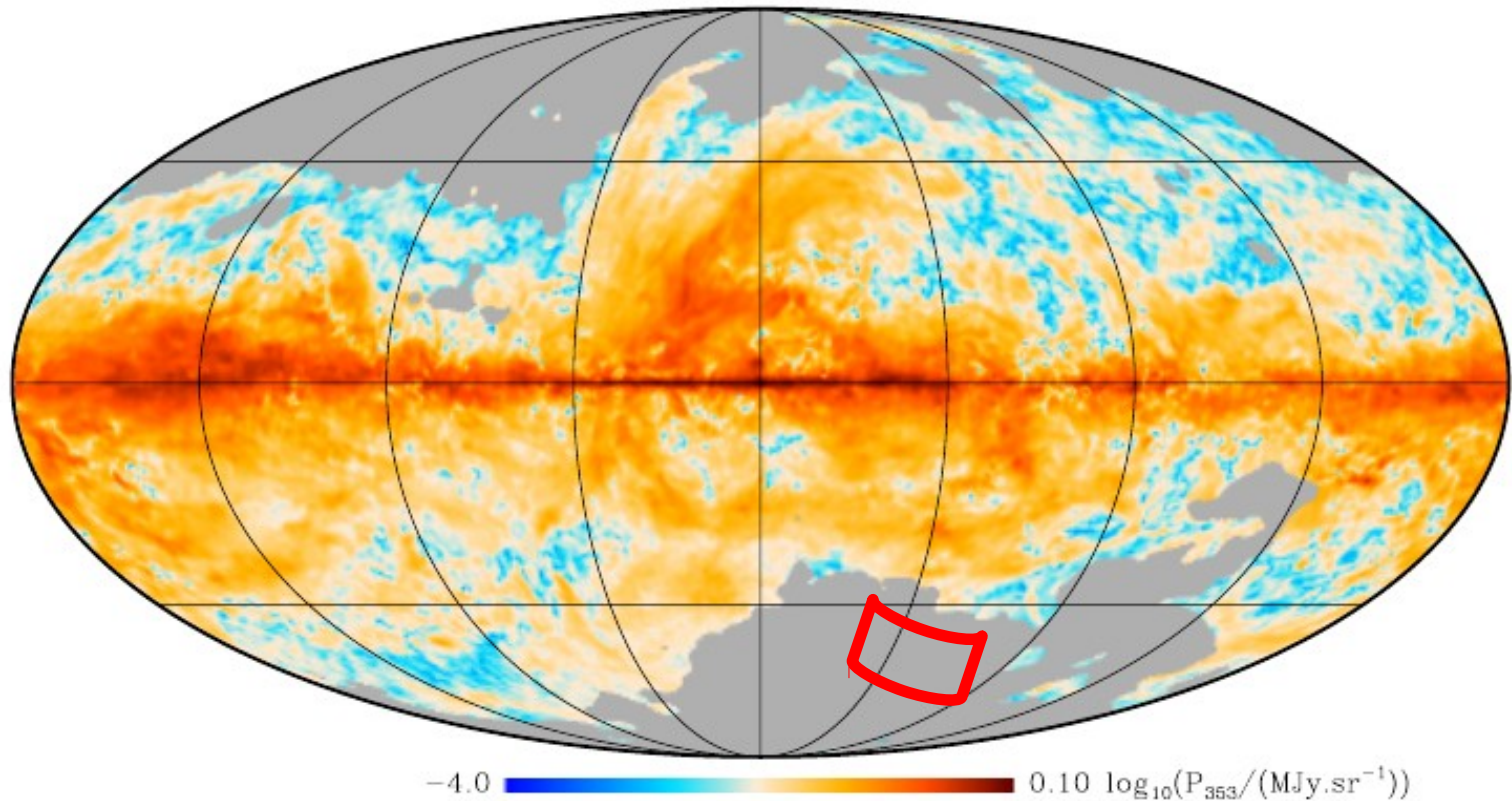
Component separation in one slide

- Foreground variables are parametrized, and fitted through:
 - Minimum variance
 - Physical parametrization (amplitude, spectral parameters)
- See Planck 2013 for reviews
- Our approaches: Stompor et al. (2009, physical parametrization), B et al. 2004 (minimum variance)
- Analytic linearization available (Errard and Stompor 2012) for forecasts

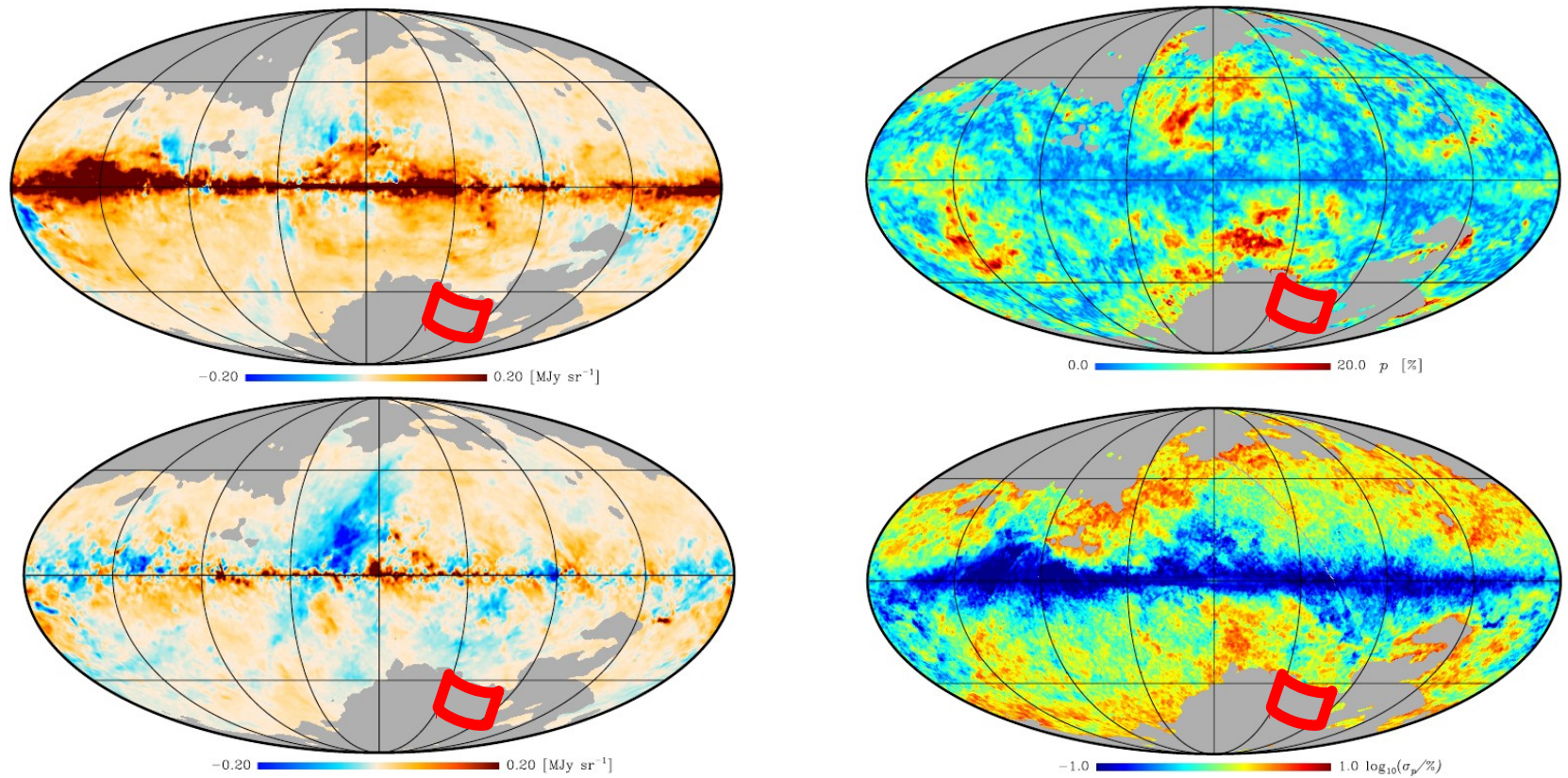
The B modes at degree angular scale



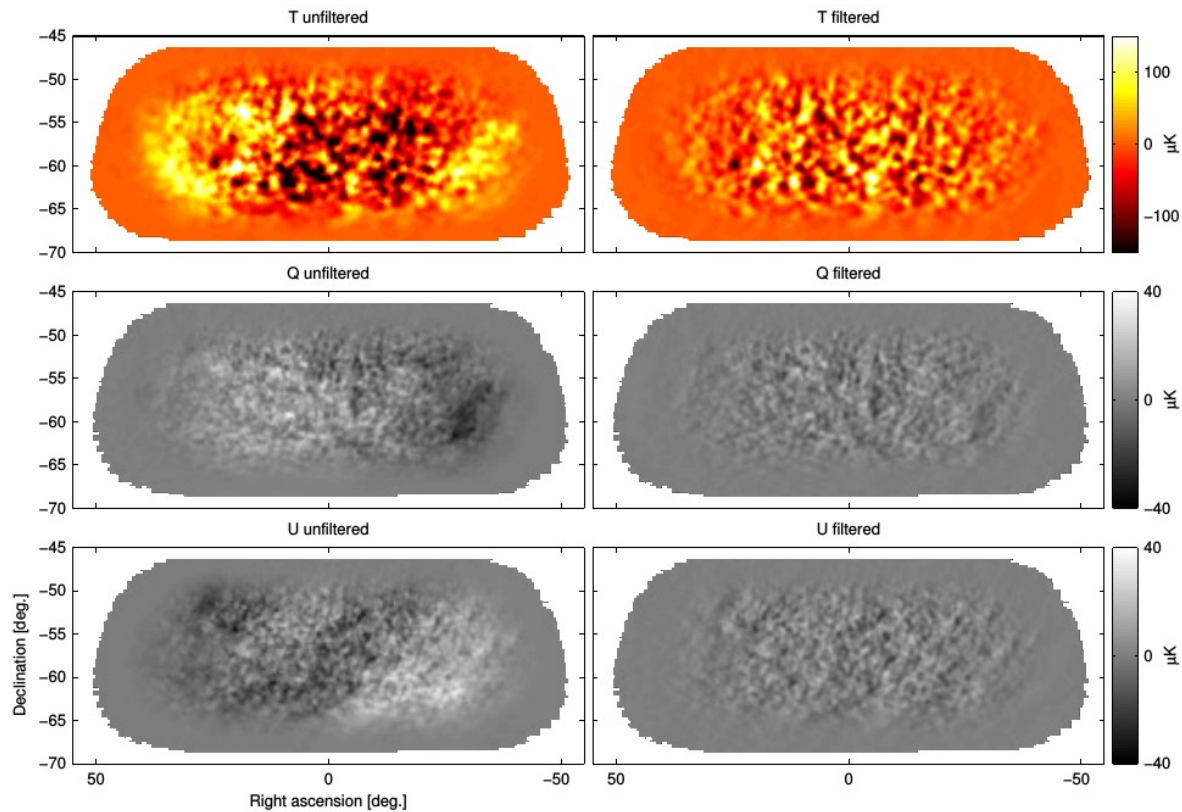
Planck observed dust polarization at intermediate latitudes



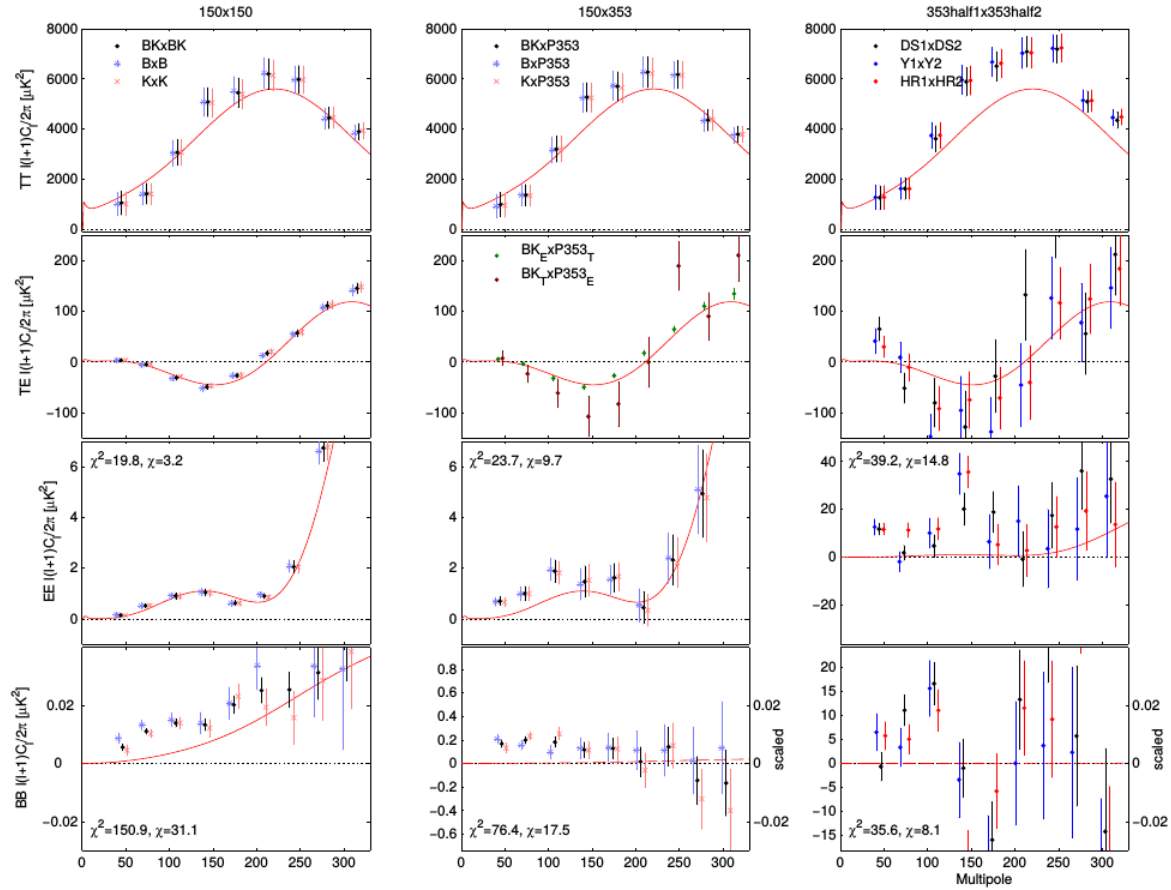
Planck observed dust polarization at intermediate latitudes



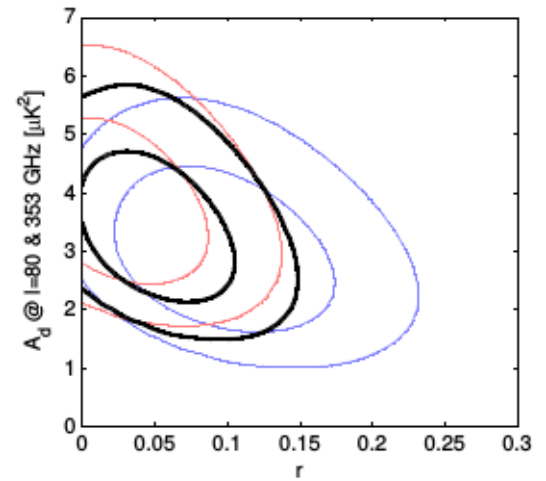
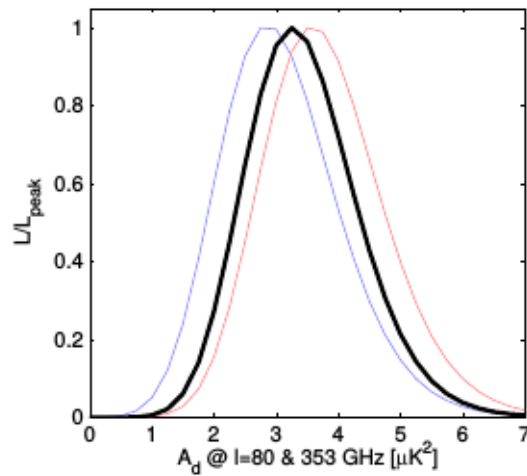
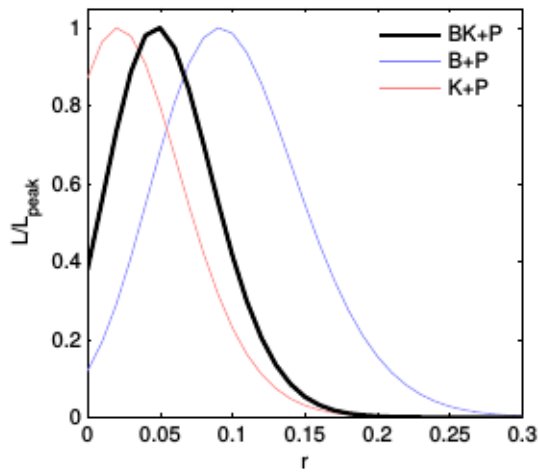
Planck × Bicep2 × KECK



Planck × Bicep2 × KECK



Planck × Bicep2 × KECK



Component separation for sub-orbital experiments

- Maximum likelihood casting, Stompor et al. 2009
- Implementation in the Miramare code, Leach e al., 2010
- Simulations of sub-orbitals, Stivoli et al. 2010
- Parameter estimation, Fantaye et al. 2011
- Power spectrum estimation through the Xpure code, Grain et al. 2012
- Foreground cleaning and lensing reconstruction, Fantaye et al. 2012
- Linearized system for forecasts, Errard and Stompor 2012